National Physical Laboratory

REPORT

NPL REPORT ENG 23

iGPS Capability Study

Ben Hughes, Alistair Forbes,
Wenjuan Sun (NPL)
and
P Maropoulos, J Muelaner,
J Jamshidi, Z Wang
(University of Bath)

February 2010

National Physical Laboratory, Hampton Road, Teddington, Middlesex, United Kingdom, TW11 0LW
Switchboard 020 8977 3222 NPL Helpline 020 8943 6880 Fax 020 8614 0446 E-mail enquiry@npl.co.uk www.npl.co.uk

The National Physical Laboratory is operated on behalf of the National Measurement Office by NPL Management Limited, a wholly owned subsidiary of Serco Group plc

iGPS Capability Study

Ben Hughes, Wenjuan Sun
Engineering Measurement Division
NPL

Alistair Forbes
Optical Technologies and Scientific Computing
NPL
&
Paul Maropoulos, Jody Muelaner, Jafar Jamshidi, Zheng Wang
IdMRC
Department of Mechanical Engineering
University of Bath

ABSTRACT

This report presents the results of testing of the Metris iGPS system performed by the National Physical Laboratory (NPL) and the University of Bath (UoB), with the assistance of Metris, and Airbus at Airbus, Broughton in March 2008. The aim of the test was to determine the performance capability of the iGPS coordinate metrology system by comparison with a reference measurement system based on multilateration implemented using laser trackers. A network of reference points was created using SMR nests fixed to the ground and above ground level on various stands. The reference points were spread out within the measurement volume of approximately 10 m × 10 m × 2 m. The coordinates of each reference point were determined by the laser tracker survey using multilateration. The expanded uncertainty (k=2) in the relative position of these reference coordinates was estimated to be of the order of 10 µm in x, y and z. A comparison between the iGPS system and the reference system showed that for the test setup, the iGPS system was able to determine lengths up to 12 m with an uncertainty of 170 µm (k=2) and coordinates with an uncertainty of 120 µm in x and y and 190 µm in z (k=2).

ISSN 1754-2987

National Physical Laboratory
Hampton Road, Teddington, Middlesex, TW11 0LW

Approved on behalf of the Managing Director, NPL
By Dr John Greenwood, Knowledge Leader, Engineering Measurement Team

1 Introduction

An experiment was undertaken at Airbus, Broughton to determine the performance capability of the Metris Indoor GPS (iGPS) coordinate measurement system (known commercially as Metris iSpace since April 2008). The experiments were performed between 25th and 28th March 2008 at Airbus, Broughton by staff from the National Physical Laboratory (NPL) and the University of Bath (UoB) with support and assistance from Metris and Airbus. This work was funded by the DIUS Measurement For Innovators programme under a Joint Industry Project (JIP) with in-kind funding from Metris and Airbus and a cash contribution from Airbus UK.

This report presents the experimental setup and procedures, data analysis and the results obtained.

1.1 Introduction to iGPS

The iGPS system is a flexible, scaleable, large volume coordinate measurement system that comprises a number of active transmitters and one or more intelligent receiver(s). The coordinates of each receiver are determined in terms of the azimuth and elevation angles from each of the transmitters. Each transmitter sweeps two fan-shaped laser beams throughout the working volume at approximately 40 rpm. The centre of the two fan-shaped beams are separated by 90° around the rotation axis and the beams are inclined by 30° either side of the vertical. An infrared strobe pulse is emitted at the start of every other rotation. Signal processing electronics associated with the receivers detect the strobe pulse and the passage of the two rotating beams. The azimuth and elevation angles between each transmitter and each receiver are determined by the relative timings of these light beam signals. Figure 1 shows an iGPS transmitter and a schematic representation of the rotating fan beams and the timing of the fan beam signals, t_1 and t_2, at the receiver relative to the strobe pulse. The horizontal and vertical angles between a transmitter and receiver pair are derived from the average of t_1 and t_2, and the difference between t_1 and t_2, respectively.

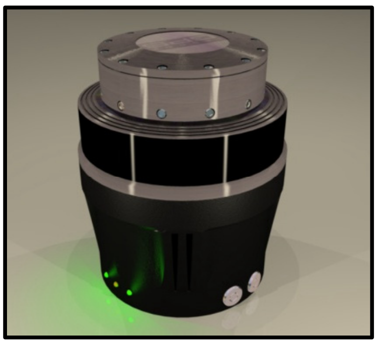

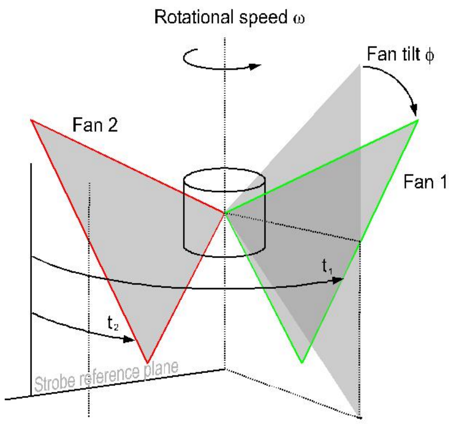

Figure 1, an iGPS transmitter (left) and a schematic representation of the rotating fan beams and their relative timing to the strobe (right).

The receiver is a cylindrical photo detector coupled to signal processing electronics.

Figure 2 Shows a Vector Bar – a combination of two receivers mounted in-line with a probing sphere – that can be used as a hand-held probe.

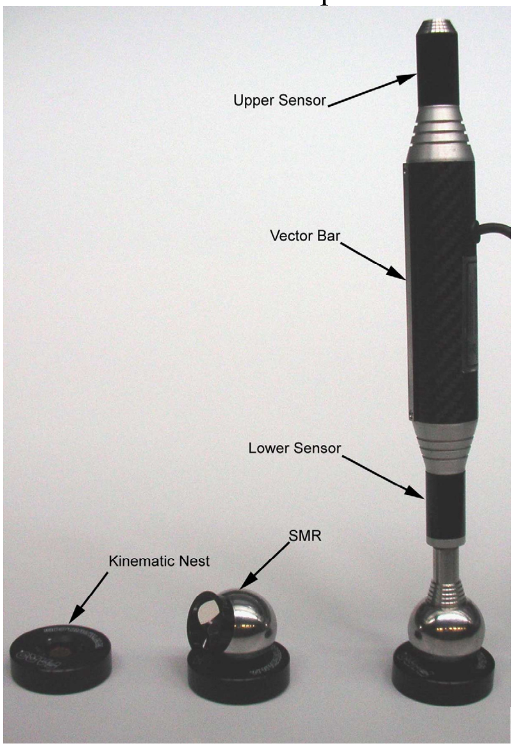

Figure 2, iGPS Vector Bar comprising two receivers in-line with a probe ball.

The position (location and orientation) of each transmitter is determined by triangulation in a similar way to the bundle adjustment procedures familiar in photogrammetry.

The iGPS/iSPACE product is sold in several standard configurations ranging from a four-transmitter, single vector bar system to an eight-transmitter system with reference receiver monuments plus multiple measurement receivers. The basic four-transmitter system uses the known distance between the two receivers on the vector bar to introduce a length scale into the system, whereas the monument based setup use the calibrated coordinates of the monuments to provide scale and a self-monitoring ability. The flexibility of the system means that any of the standard configurations can be extended by adding more transmitters and/or receivers as necessary to improve accuracy, volume, or coverage.

1.2 Objectives

The objectives of the work described in this report were to

- compare the performance of the iGPS system with a reference system,
- establish a reference uncertainty model for iGPS that could make reliable predictions of iGPS system performance
- validate the model by comparing the model predicted behaviour of the system with that achieved in practice, and
- produce a good practice guide for deployment and use of iGPS.

In this way a reliable statement of iGPS performance capability for any configuration could be made.

In reality, some of these objectives have not been met within the current project. See Section 5 for a discussion. However, the main customer requirement - a statement of the measurement capability of the iGPS system as tested - has been achieved.

1.3 Testing methodology

The philosophy adopted to test the system was to establish an array of (twenty-four) reference points with very accurately known coordinates along with corresponding coordinate uncertainties. The reference points were located using data obtained from several laser tracker surveys. The surveys were taken from different locations around the volume and the data combined using NPL's optimised multilateration software [1]. This software fits the complete set of coordinate data produced by the tracker measurements in a weighted non-linear least-squares adjustment to determine estimates of the relative positions of each tracker as well as estimates of the reference point coordinates in a fixed frame of reference. This software also produces the required variance matrix associated with the coordinates from which uncertainties associated with reference point coordinates and distances between reference points can be evaluated.

The reference points were then surveyed using the iGPS system and the results compared with the reference results.

The most robust way to compare different sets of coordinate is to fit one set to the other using a weighted, non-linear least-squares fitting algorithm where the weights are derived from the estimated uncertainty of each point measurement [2,3]. Ideally, a measuring system would provide the estimated uncertainty of each coordinate in the form of a variance matrix as part of the measurement output, as is the case with the NPL multilateration software. In the case of the iGPS system the variance matrix associated with the measured data was not provided by the system, so a standard least-squares fit was used instead. This model is described in more detail in section 2.1.

The weighted non-linear least-squares approach was employed when dealing with the laser tracker data and statistical tests were performed on the fitted data to validate the variance matrix and hence the uncertainty model used to represent the laser tracker.

In addition to measurements of the reference points, a second test was performed to investigate the reproducibility of the iGPS setup by measuring the length of a carbon fibre scale bar fitted with iGPS receivers at both ends. The scale bar was moved to different locations and orientations within the measurement volume and its length at each position measured using the iGPS system.

The iGPS system was set up and calibrated by Metris using a monument network that was calibrated using a laser radar. The reference coordinates were established by NPL and UoB using two laser trackers and multilateration. The iGPS measurements were carried out by Metris with NPL/UoB observing. The availability of the laser radar gave us the opportunity to survey the reference point using a third instrument. All measurement results were openly exchanged between NPL/UoB and Metris.

In the following sections, section 2 describes the reference uncertainty model developed for the iGPS and laser tracker systems and the uncertainty performance predicted by these models. Section 3 describes the experimental setups and the measurement procedures in more detail and section 4 contains a description of the data analysis and the results of the experiments. Some of the issues encountered during the delivery of this work are described in section 5.

2 Reference uncertainty models

Two uncertainty models were developed; one to represent the uncertainties associated with the laser tracker, and one for iGPS sensor data. In both cases, the instruments were regarded as "black-boxes" *i.e.* the inner workings were not modelled, instead, the models simply represented the type of data generated by the systems. In the case of the laser tracker, this data is in the form of a distance and two angles. For the iGPS system, the data is in the form of an azimuth and elevation angle between each transmitter and each receiver. The models are described below.

2.1 Uncertainty model and predictions for iGPS-type measurements

We have used a mathematical model to predict the uncertainty associated with target coordinates from the angle data. The model assumes that the angle measurements are subject to independent, normally distributed random effects according to the model

$$\theta = \theta^* + \varepsilon, \qquad u^2(\varepsilon) = \sigma_A^2 + \sigma_B^2 / d^2,$$

where θ^* is the true angle, θ is the measured angle, ε is a random effect with uncertainty $u(\varepsilon)$ that depends on the distance d from the station to the target. This uncertainty depends on two statistical parameters σ_A and σ_B, the latter specifying the dependence on the transmitter-receiver distance. The model also assumes that all transmitters see all the receivers.

In addition, an iGPS system requires further scale-setting calibration information, for example:

- calibration of the vector bar,
- measurement of a calibrated scalebar,
- measurement of a calibrated set of monuments.

The reference model caters for all three (and combinations of them, if required). In the results discussed below, it was assumed that the calibration information was provided through a set of calibrated monuments; see section 3.1.

The model was used to predict the uncertainty associated with the measured coordinates of the probe centre of a vector bar. The model has two variants, relating to how the vector bar is modelled;

1. The vector bar is treated as a rigid body with the probe centre and two targets at known distances along a single axis,
2. The two targets are measured independently and from these an estimate of the probe centre is derived.

The first model will, in general, provide more accurate estimates of the probe location.

Figure 3 gives the predicted uncertainties (k=1) associated with the inter-target distances derived from the reference model for the case $\sigma_A = 1''$ (one arc-second) and $\sigma_B = 0.1$ mm (with distances d measured in mm) applying equally to azimuth and elevation angles. The vector bar was modelled as having receivers 50 mm and 150 mm from the probe centre. Figure 4 gives the corresponding predicted uncertainties (k=1) associated with the target coordinates. For the model variant in which the vector bar is treated as a rigid body, the predicted uncertainties associated with the z-coordinates are significantly less than those corresponding to the x- and y-coordinates. For the other model variant, the estimates of the z-coordinates are still more accurate than other two coordinate estimates. This is to be expected given the relatively low height of the measuring volume compared to its width. Figure 5 and Figure 6 give predicted uncertainties corresponding to the case $\sigma_A = 1''$ and $\sigma_B = 0.15$ mm.

For either model variant, the reference model (as implemented) predicts that for the particular transmitter-receiver configuration, the uncertainties in the z-coordinates should be less than those associated with the other two coordinates. The observed results described in section 4.2.2 suggest that the observed z-coordinate data is less accurate. The reason for this is not yet understood. One explanation for this could be that the elevation angle measurements are less accurate than the azimuth angle measurements, or the presence of correlation between azimuth and elevation angle estimates (not unlikely since both are derived from the same set of time measurements.)

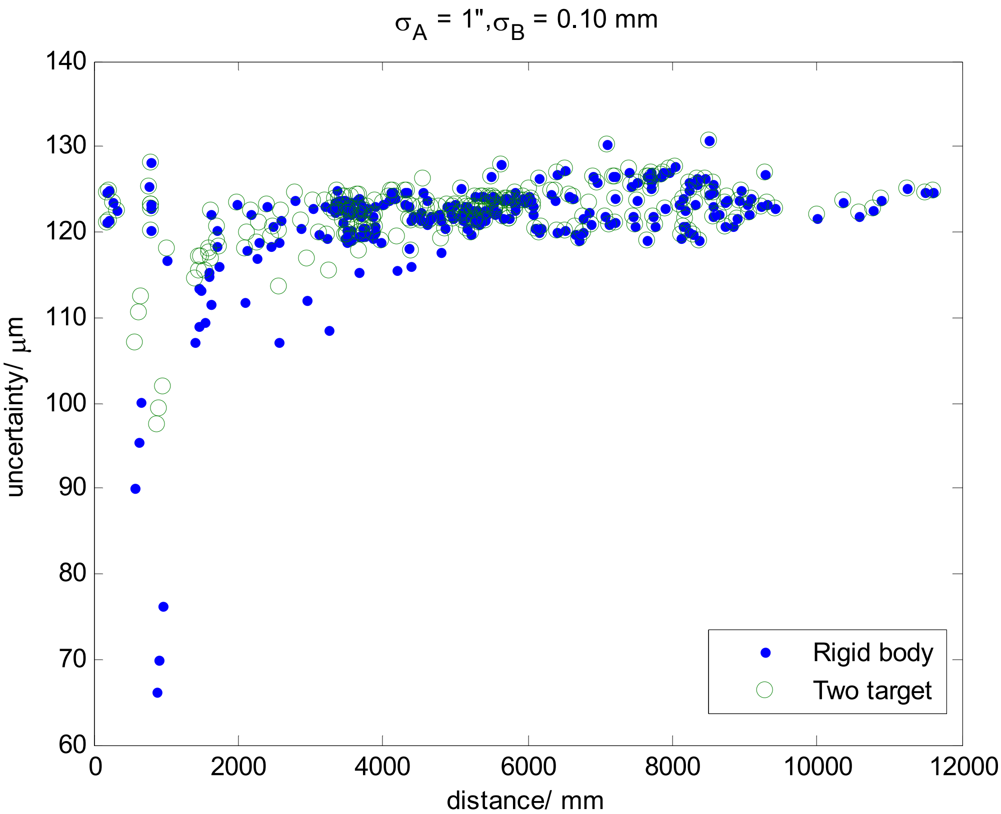

Figure 3. Predicted uncertainties (k=1) associated with inter-target distances derived from the reference model.

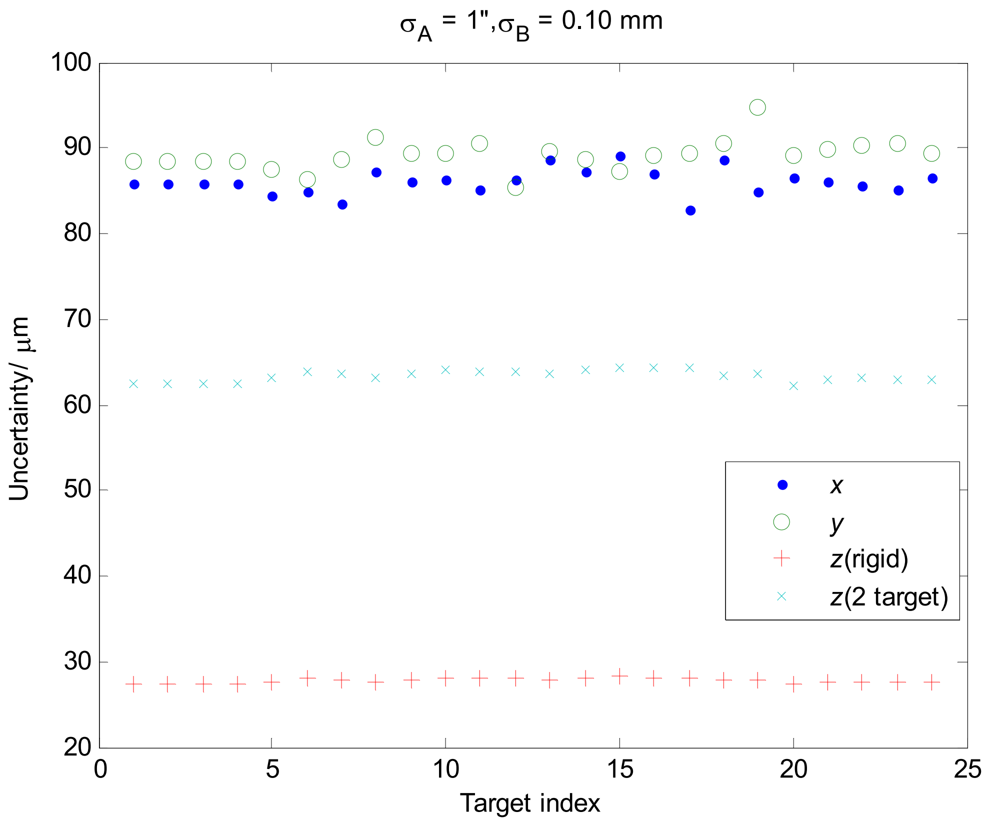

Figure 4. Predicted uncertainties (k=1) associated with target coordinates derived from the reference model.

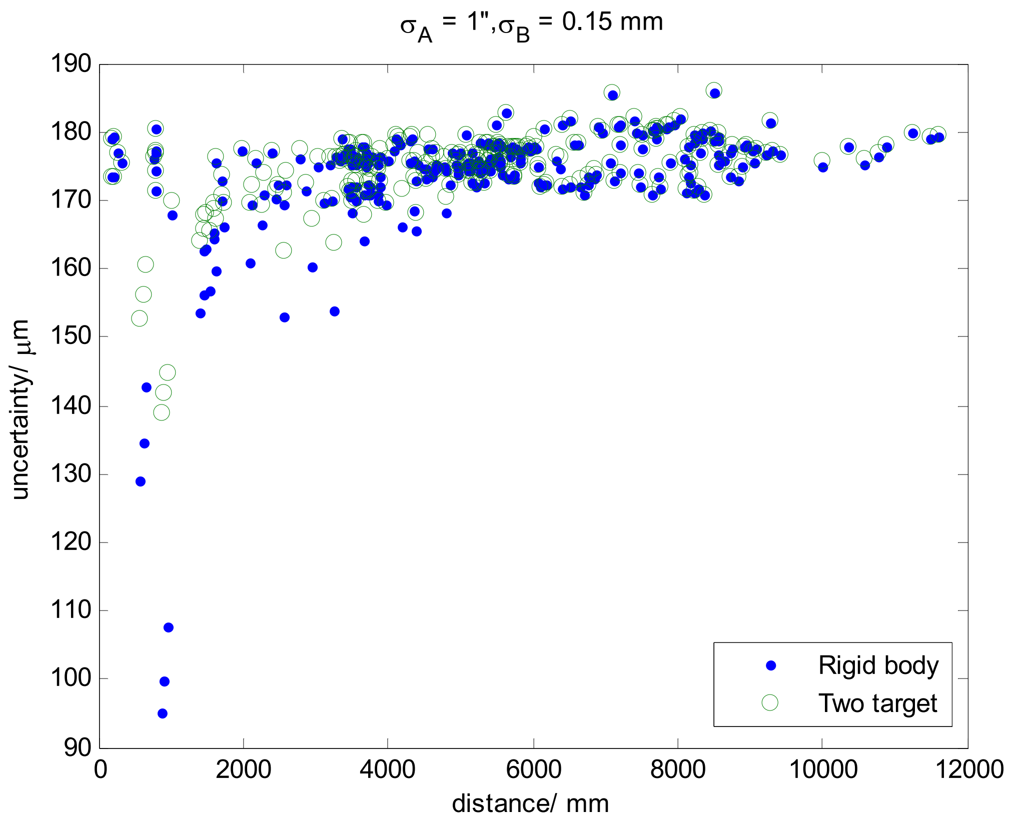

Figure 5. Predicted uncertainties (k=1) associated with inter-target distances derived from the reference model.

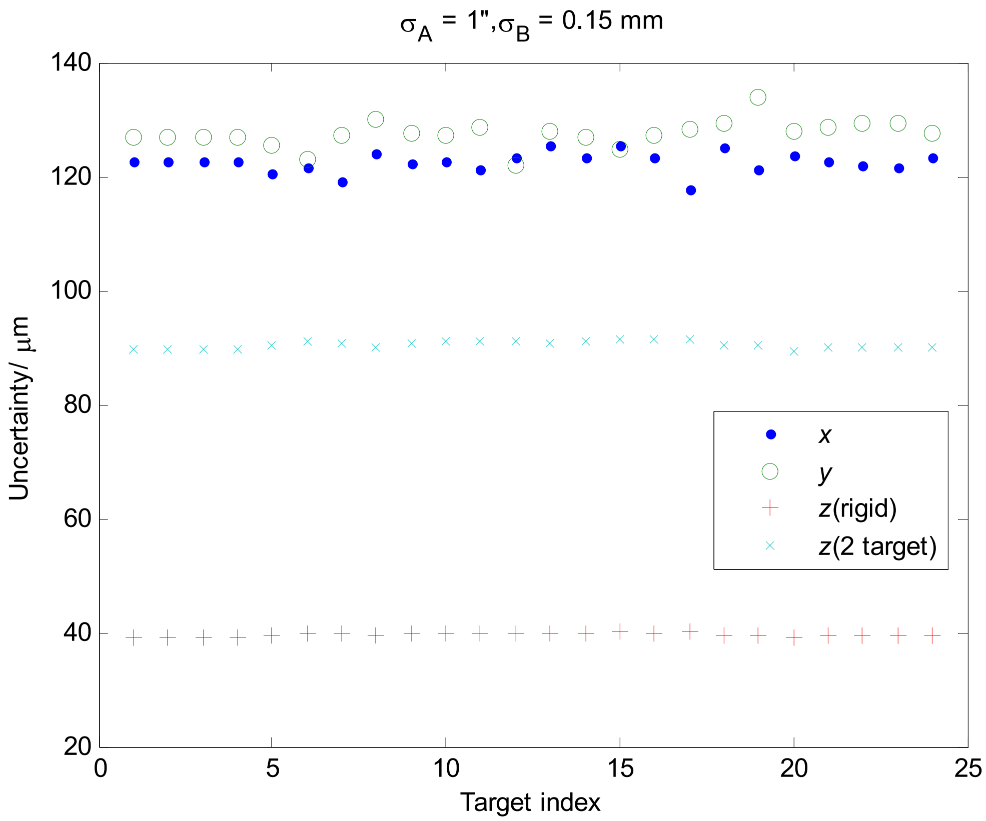

Figure 6. Predicted uncertainties (*k*=1) associated with target coordinates derived from the reference model.

2.2 Extensions to the reference model

The NPL reference model, as initially designed, treated the iGPS system as a type of theodolite system in which azimuth and elevation angles of nominally fixed targets are gathered from nominally fixed station locations, with scale information set by measurements of a calibrated scale bar. The iGPS system can operate in this mode. The actual system tested operated differently. A vector bar was used as the primary probing device so the system had to be remodelled as gathering angle measurements of a two-target rigid body in different positions.

A second improvement to the model involved the use of the monuments. In the standard reference model, the station locations are regarded as fixed but unknown, to be determined as part of the solution process. If the stations drift during the measuring process the result will be a loss of accuracy in the computed target locations. In the monument-based system, each time a target is measured, the monument locations are also measured and the station positions recomputed along with the location of the target. As a consequence, the target locations are determined relative to the monuments with the station positions calculated as intermediate quantities. The advantage of this approach is that the target location estimates do not depend strongly on the stability of the station positions, only on stability of the monument locations. Incorporating the monument approach involved a significant (but very useful) extension of the reference model.

2.3 Reference model for Laser Tracker measurements

A laser tracker measurement gives the estimates of the target coordinates in terms of distance and angle measurements $\mathbf{s}_i = (r_i, \theta_i, \phi_i)$ according to

$$\mathbf{x}_i = (r_i \cos\theta_i \cos\phi_i, r_i \sin\theta_i \cos\phi_i, r_i \sin\phi_i) .$$

If $\mathbf{s}_i^* = (r_i^*, \theta_i^*, \phi_i^*)$ are the true distance and angles associated with true coordinates $\mathbf{x}_i^*$, so that $r_i^* = \|\mathbf{x}^*\|$, $\theta_i^* = \tan^{-1}(y_i^* / x_i^*)$, $\phi_i^* = \sin^{-1}(z_i^* / r_i^*)$, then a simple model of the random and systematic effects associated with the measurements $\mathbf{s}_i$ is given by

$$r_i = r_i^*(1 + d_\mathrm{R} + e_{i,\mathrm{R}}) + d_\mathrm{A} + e_{i,\mathrm{A}}, \quad \theta_i = \theta_i^* + e_{i,\mathrm{H}} \quad \text{and} \quad \phi_i = \phi_i^* + e_{i,\mathrm{V}} .$$

Subscription *R*, *A*, *H*, *V*, refer to radial, azimuth, horizontal and vertical. Here $\mathbf{d} = (d_\mathrm{R}, d_\mathrm{A})$ are effects common to all the measurements and represent fixed offsets associated with the refractive index and laser deadpath. The effects $\mathbf{e}_i = (e_{i,\mathrm{R}}, e_{i,\mathrm{A}}, e_{i,\mathrm{H}}, e_{i,\mathrm{V}})$ are random effects that vary from point to point.

This model was used with appropriate values of **d** and $\boldsymbol{e_i}$ to weight the laser tracker data when calibrating the reference point network.

3 Experimental Setup & Procedure

Equipment:

- 8 × iGPS transmitters (Rev H)
- 12 × iGPS fixed monuments (comprising iGPS receiver + tooling balls for calibration)
- 1 × Metris mini vector bar
- 1 × Metris Laser Radar
- 2 × FARO Xi Laser Trackers
- 2 × ½ inch Spherically Mounted Retroreflector (SMR)
- SMR nests
- 1.5 m Carbon Fibre Scale Bar fitted with iGPS receivers
- Tooling balls
- Metris "Surveyor" software (the basis of the iSpace software package)
- Spatial Analyser software

The experimental setup is shown in Figure 7. The components of the setup and the measurement procedures are described below.

3.1 iGPS setup and calibration

The eight iGPS transmitters were arranged in a square with a transmitter at each corner and half way along each side. The transmitters were mounted on tripods with the corner transmitters mounted higher than those on the sides of the square. Associated with each transmitter was a receiver monument, which was also mounted on a tripod close to and either above or below each transmitter. A close up picture of a transmitter/receiver monument pair is shown in Figure 8. Four additional receiver monuments were positioned in a square around the centre of the measurement volume. These receiver monuments appear as short black pillars in Figure 7. This configuration is known as the iSpace 8i configuration – the most accurate of the standard configurations.

The iGPS system was calibrated by Metris using the receiver monuments and a laser radar. Each monument comprised four tooling balls and an iGPS receiver as shown in Figure 9. The relative positions of the tooling balls and receiver on each monument were previously established by Metris. The position (location and orientation) of each receiver monument was established by laser radar survey. Each tooling ball was measured using the laser radar from multiple laser radar positions around the working volume. The laser radar data along with the individual monument calibrations was then processed using the bundle adjustment algorithms in Spatial Analyser to yield the receiver position for each monument.

The receivers were then surveyed using the iGPS system. The resulting data was processed by Metris software to establish the position of each iGPS transmitter.

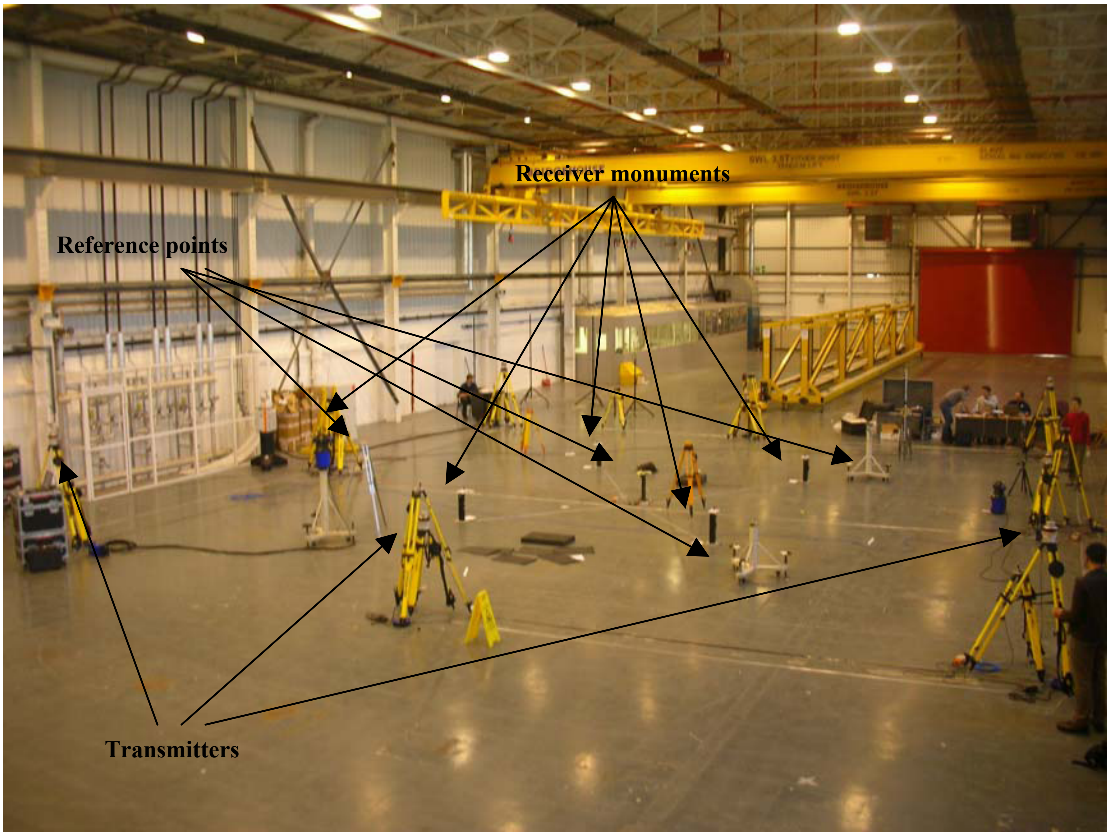

Figure 7. The experimental setup showing eight iGPS transmitters on yellow tripods, twelve receiver monuments and twenty-four reference points.

Figure 8. Close up of a transmitter/receiver monument pair.

Figure 9. Receiver monument comprising four tooling balls and an iGPS receiver.

3.2 Reference Point Network Setup and Calibration

The reference point network was constructed by fixing twenty-four SMR nests to the floor, three tripods, an aluminium post and two theodolite stands using a hot-glue gun. The reference points were spread out within a volume of approximately 10 m × 10 m × 2 m. The position of each reference point was measured using two laser trackers operated simultaneously to reduce measurement time. Each tracker was used to survey the reference points from multiple positions around the working volume. One tracker was mounted relatively high on a tripod. The other was mounted at ground level. The trackers were set up to operate in “Interferometer set by ADM” mode. Each tracker position was chosen carefully to ensure that all reference points were visible to the tracker. Each SMR nest was wiped clean prior to mounting the SMR to reduce the risk of dust affecting the measurements.

A total of twenty-six surveys from eight tracker positions were obtained. The data was combined using an NPL developed multilateration algorithm and the weighting scheme based on the laser tracker reference model described in section 2.3 to determine the reference point coordinates and their associated uncertainties.

The data was further processed to separate the shape uncertainty from the rigid-body position uncertainty for the data set. In other words, any uncertainty contribution arising from defining a fixed frame of reference associated with experimental setup was removed to leave just the uncertainty components relevant to “shape” of the reference point network [2].

The residuals of the fitting process were analysed to ensure statistical consistency, to verify the laser tracker uncertainty model and hence the coordinate measurement uncertainty.

3.3 Scale Bar Measurements

The scale bar test was intended to show the *reproducibility* of the iGPS system and highlight any sensitivity to inclination of the receiver relative to the transmitters. A 1.5 m carbon fibre scale bar fitted with a receiver at each end was fitted to a tripod as shown in Figure 10.

Figure 10. Scale Bar.

The tripod was positioned at three locations within the measurement volume. At each location, the scale bar was rotated in steps about the vertical and horizontal axes. The length of the scale bar was measured by the iGPS system at each of twenty-nine scale bar positions. The range of orientations at which the scale bar was measured is shown in Figure 11.

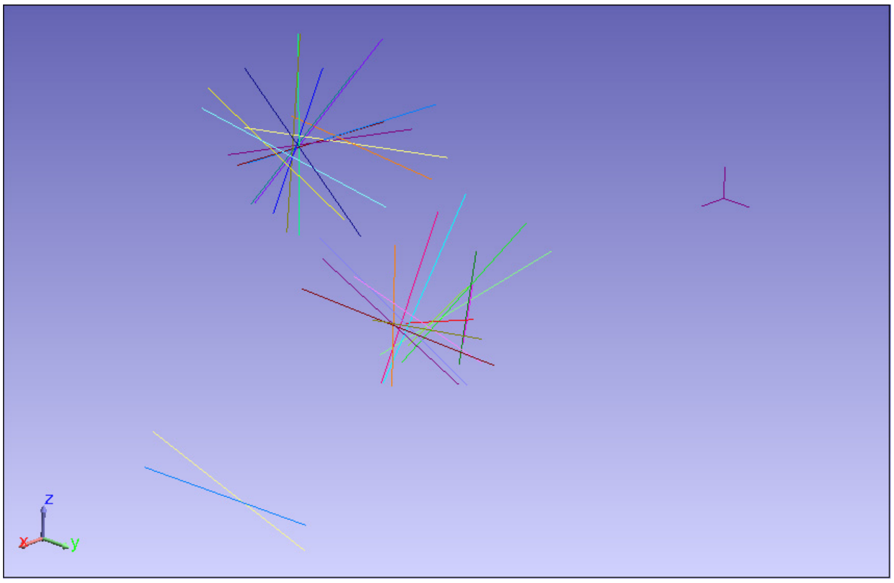

Figure 11. Positions and orientations of the scale bar.

Note that for this test, the scale bar was not calibrated. The objective was to investigate any variation in measured length due to position and orientation of the receivers within the measurement volume.

4 Data Analysis And Results

The *ideal* data analysis associated with the four main stages of this experiment is illustrated in Figure 12. In this figure, measurement processes are shown in purple, measured data in pink, calculations in yellow and calculated data in green. Figure 12 also shows model assumptions in light blue.

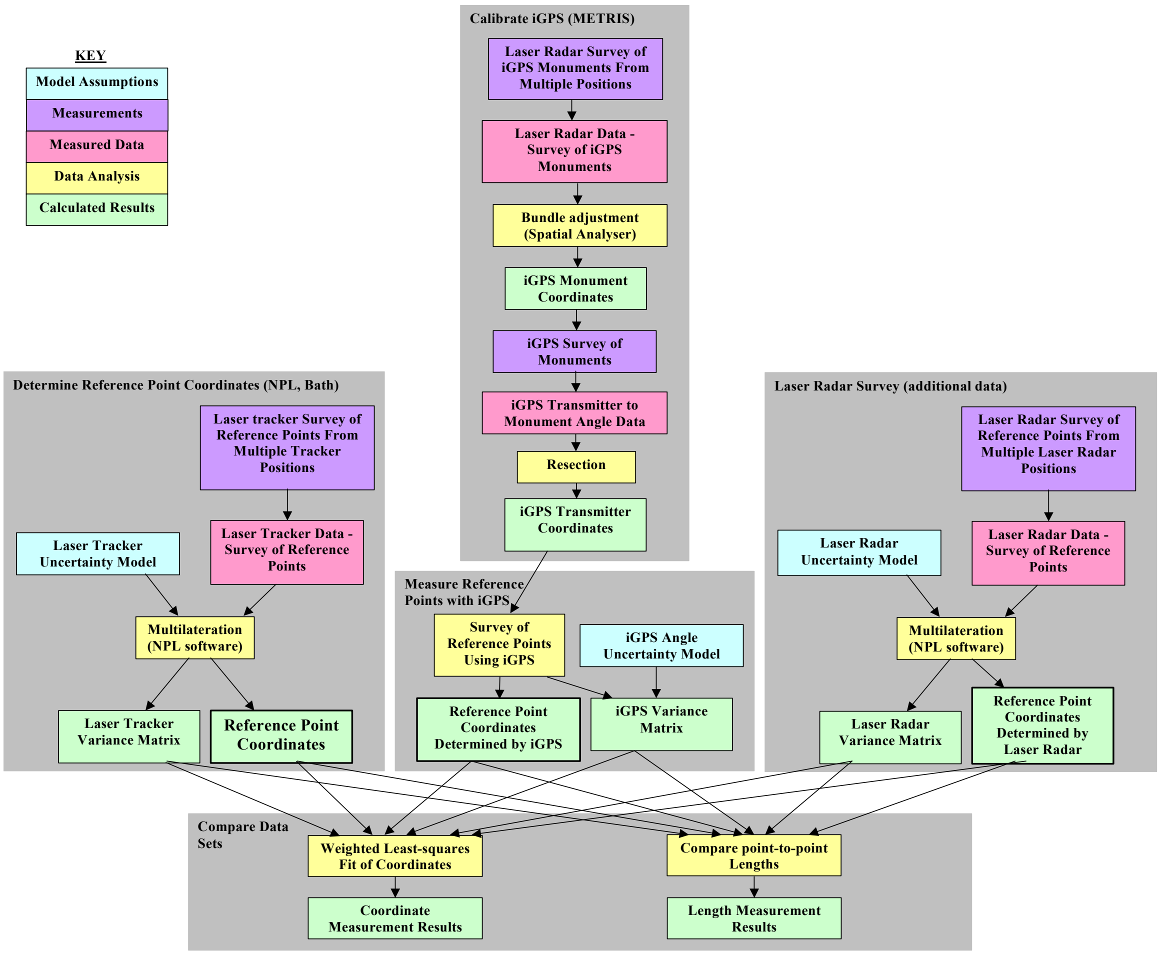

Figure 12. Flow chart of data acquisition and analysis.

In the box labelled "Measure Reference Points with iGPS in the middle of Figure 12, the variance matrix associated with the iGPS observations is computed based on an uncertainty model. As will be shown later, the iGPS model described in section 2 does not explain some aspects of the observed data. The NPL reference model is designed to cater for a wide range of coordinate metrology systems, including multilateration, theodolite and laser tracker systems. The reference model implements an iGPS system as type of theodolite system, which, in practice, is an oversimplification. The iGPS system has a high level of systematic error compensation that results in significant residual sources of systematic uncertainty that are not accounted for in a theodolite-type model. The uncertainties predicted from the NPL reference model for the iGPS system should therefore be regarded as providing only a baseline for comparison purposes. In this report, the algorithms comparing iGPS and tracker measurements use only the point coordinates in an un-weighted least squares matching algorithm.

4.1 Reference Point Network Measurements

4.1.1 Determination of Reference Point Coordinates

The reference point coordinates were computed from the laser tracker data using a multilateration approach. This method performs a weighted non-linear least-squares fit of all the sets of data to establish the reference coordinates $Y_{\mathrm{T}} = \{\mathbf{y}_j, j = 1,\ldots,24\}$ and their corresponding uncertainties in a fixed frame of reference. The weighting scheme employed put a significantly higher weight on the interferometric displacement data than on the angle data obtained from the tracker. This reflects the fact that the interferometer readings are inherently more accurate than the angle data. The weighting scheme also took into account the likely uncertainty in the refractive index estimates and those for the laser deadpath or “bird bath” distances.

Standard nonlinear least squares fitting algorithms do not cope well with outliers. A modified approach – robust least squares algorithms – was used to accommodate any outlying data. Figure 13 shows the residuals associated with the displacement measurements for the laser tracker survey. Some measurements seem discrepant. Figure 14 shows the residuals associated with the azimuth angle measurements while Figure 15 graphs those associated with the elevation angle measurements. The discrepant data is associated with the measurement of target 20 in the first laser tracker position and target 2 in the fifth position. With these measurements removed, the displacement and azimuth angle residuals are as in Figure 16 and Figure 17, respectively.

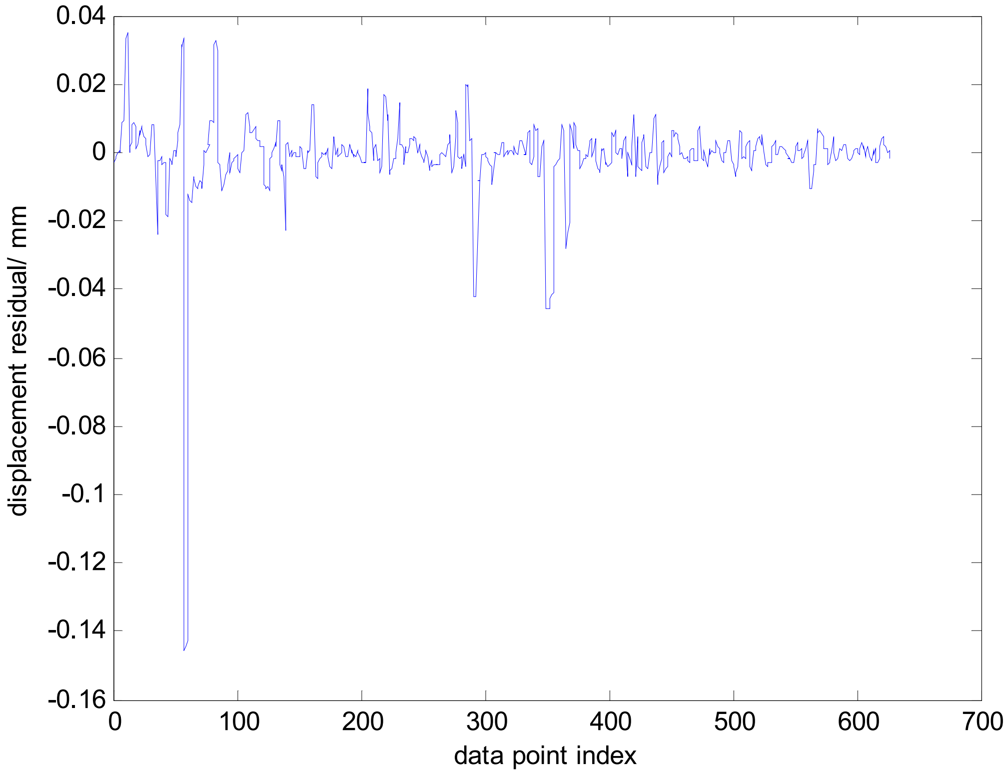

Figure 13. Residuals associated with the displacement measurements for the laser tracker survey in a robust least squares bundle adjustment.

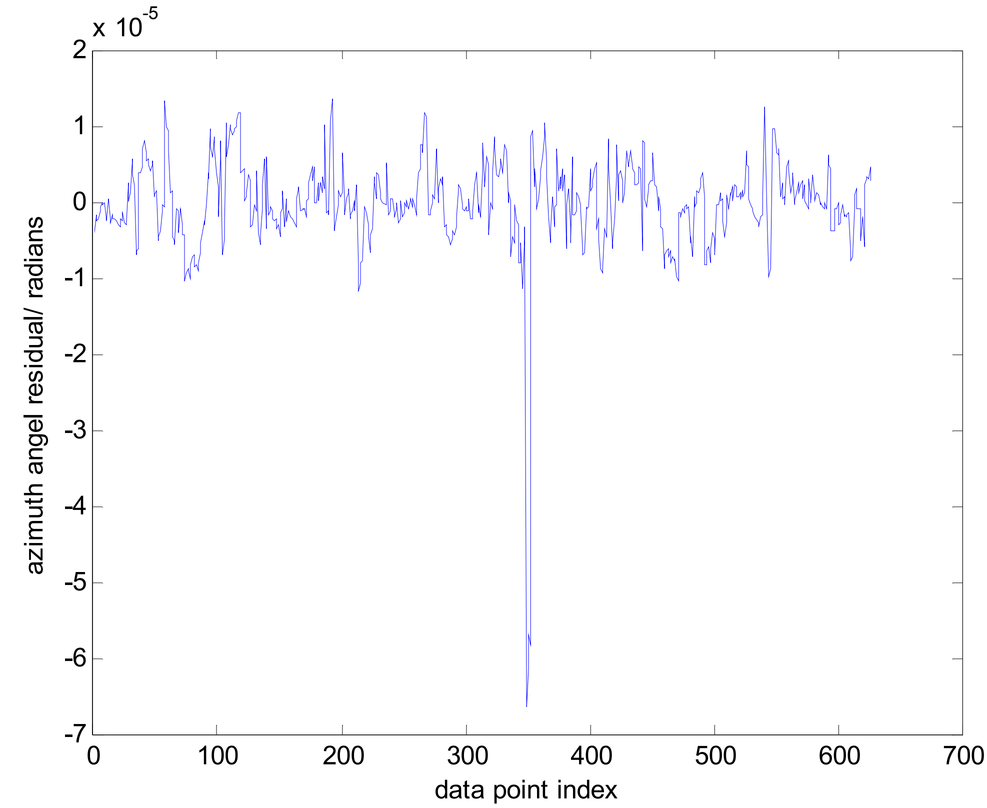

Figure 14. Residuals associated with the azimuth angle measurements for the laser tracker survey in a robust least squares bundle adjustment.

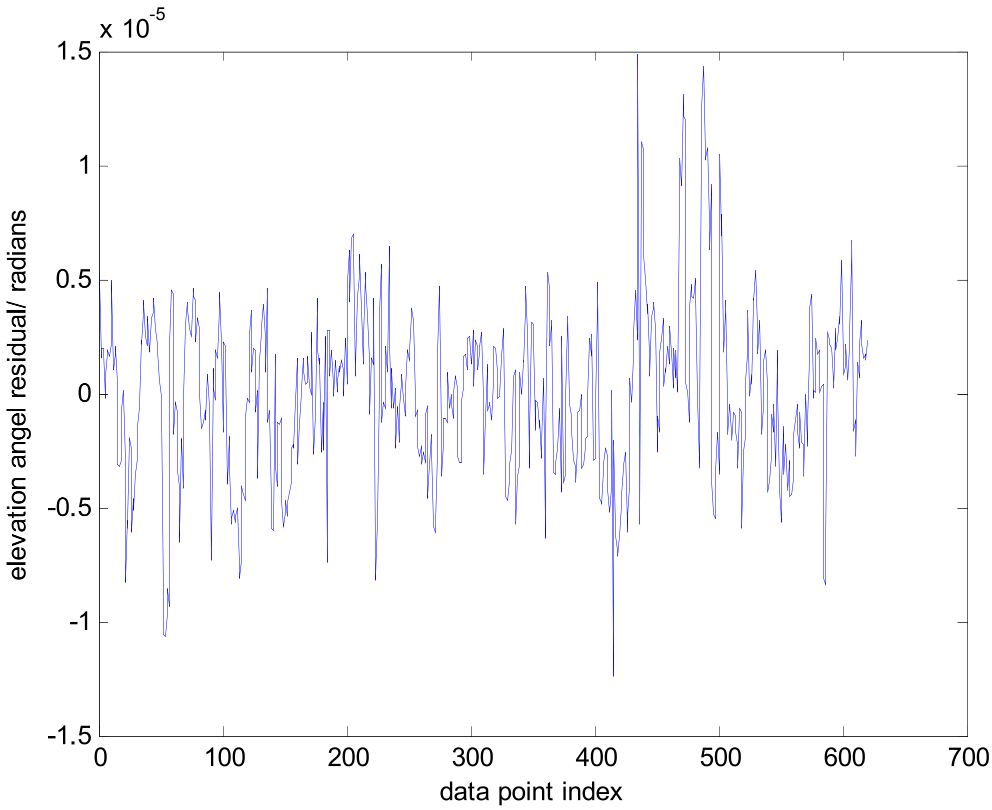

Figure 15. Residuals associated with the elevation angle measurements for the laser tracker survey in a robust least squares bundle adjustment.

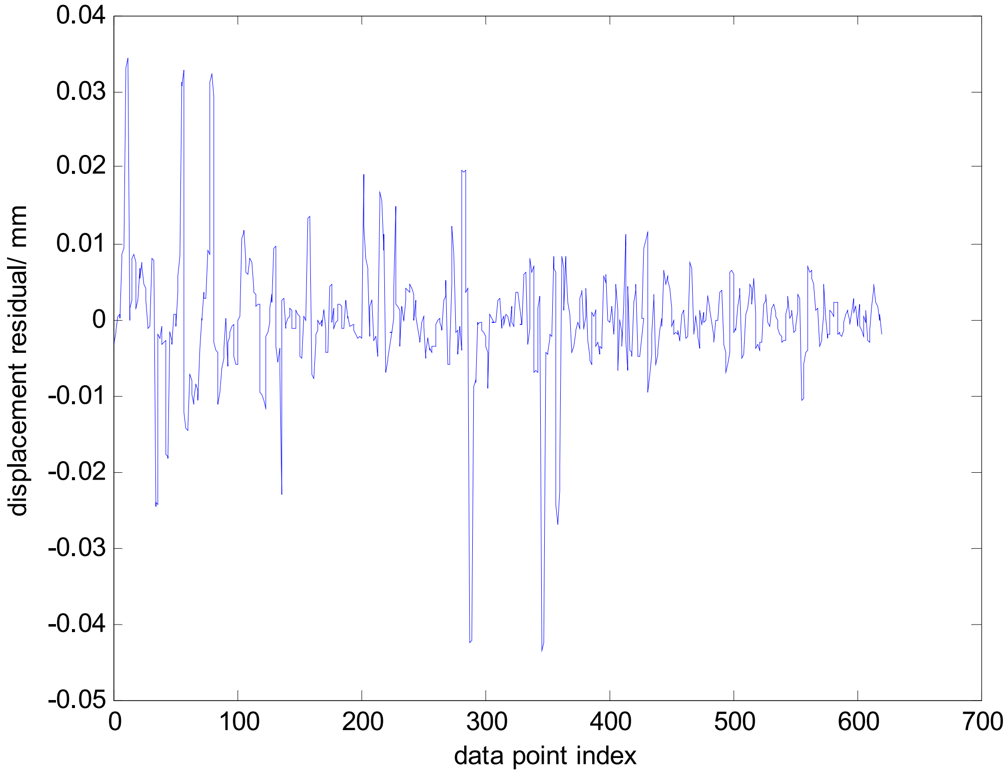

Figure 16. Residuals associated with the displacement measurements for the laser tracker survey in a robust least squares bundle adjustment, following the removal of measurements of target 20 in first tracker position and target 2 in fifth tracker position.

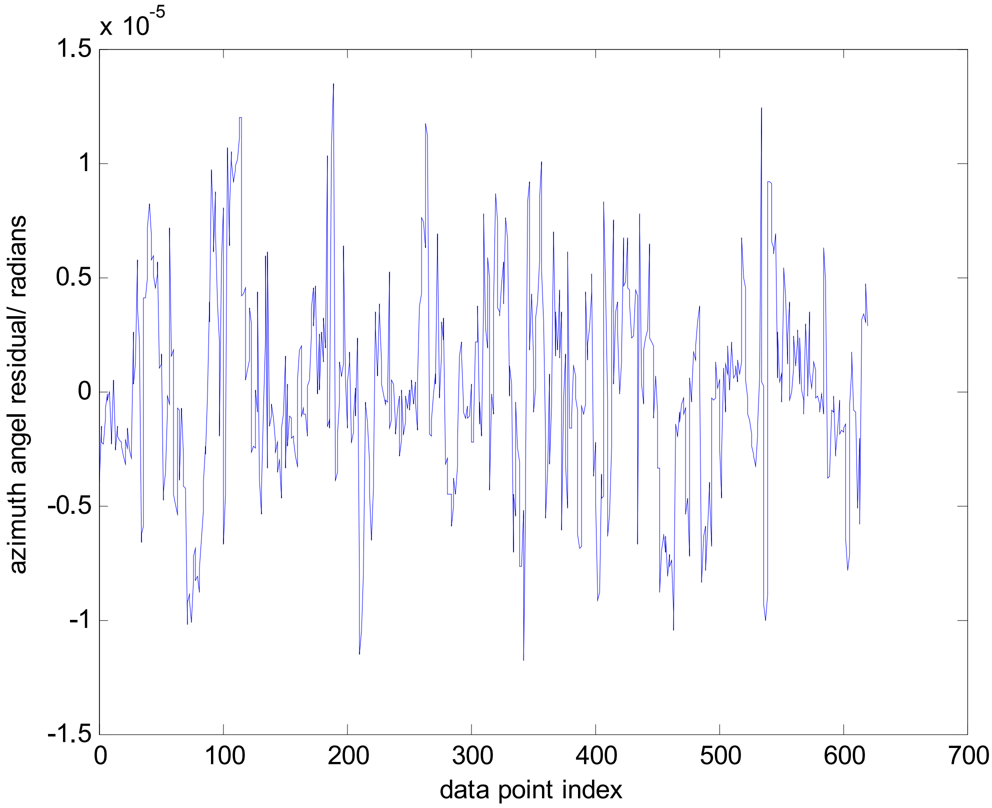

Figure 17. Residuals associated with the azimuth angle measurements for the laser tracker survey in a robust least squares bundle adjustment, following the removal of measurements of target 20 in first tracker position and target 2 in fifth tracker position.

We can assess the degree of normality for the residuals associated with tracker survey. If we do so, we find that the residuals have a larger kurtosis (of the order of 4) rather than the expected value of 3 for a Gaussian distribution. This means that there are more residuals further from the mean than would be expected. An explanation for this could be movement of the targets between tracker measurements leading to some outliers. However, even if the random effects have a Gaussian distribution, there is no guarantee that the residuals will follow the same distribution due to the effects of leverage: some sensor measurements are important in determining the model fit and will be associated with small residuals while some measurements will be ignored. It is straightforward to simulate examples of tracker surveys where the residuals have a high kurtosis but all effects follow Gaussian distributions.

The weighting scheme is based on a prior model of the likely accuracy of the angle and displacement measurements. On the basis of the residual errors of the fit, the input uncertainties were scaled so that the sum of the squares of the weighted residuals errors is equal to its expected value (the number of degrees of freedom). The uncertainties associated with the target coordinates were calculated using a *posteriori* scaling of the uncertainty information.

The variance matrix associated with the reference point coordinates was further processed to remove systematic effects that represented common, or rigid-body, uncertainty contributions to the estimated uncertainty of each point coordinate. The final point coordinate uncertainties calculated from this modified variance matrix represent the uncertainty in the shape of the point set. The expanded uncertainties are given in Figure 18 while the uncertainties associated with the inter-target distances are show in Figure 19. The measurement results indicate that the target locations have been determined to accuracy of the order of 10 µm (k = 2) in each coordinate and that the uncertainties associated with the inter-target distances are of a similar order. On this basis, the calibration of the reference point network using the tracker survey was judged to be accurate enough to test the iGPS system.

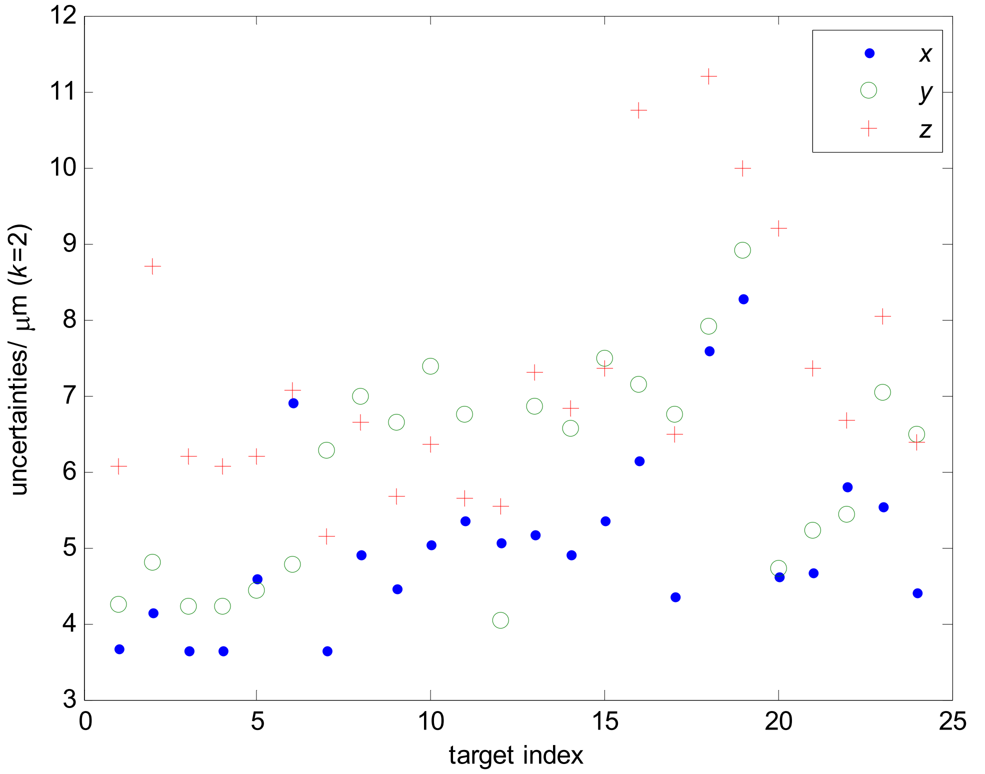

Figure 18. Expanded uncertainties (*k*=2) associated with the coordinates of the targets determined by the laser tracker survey.

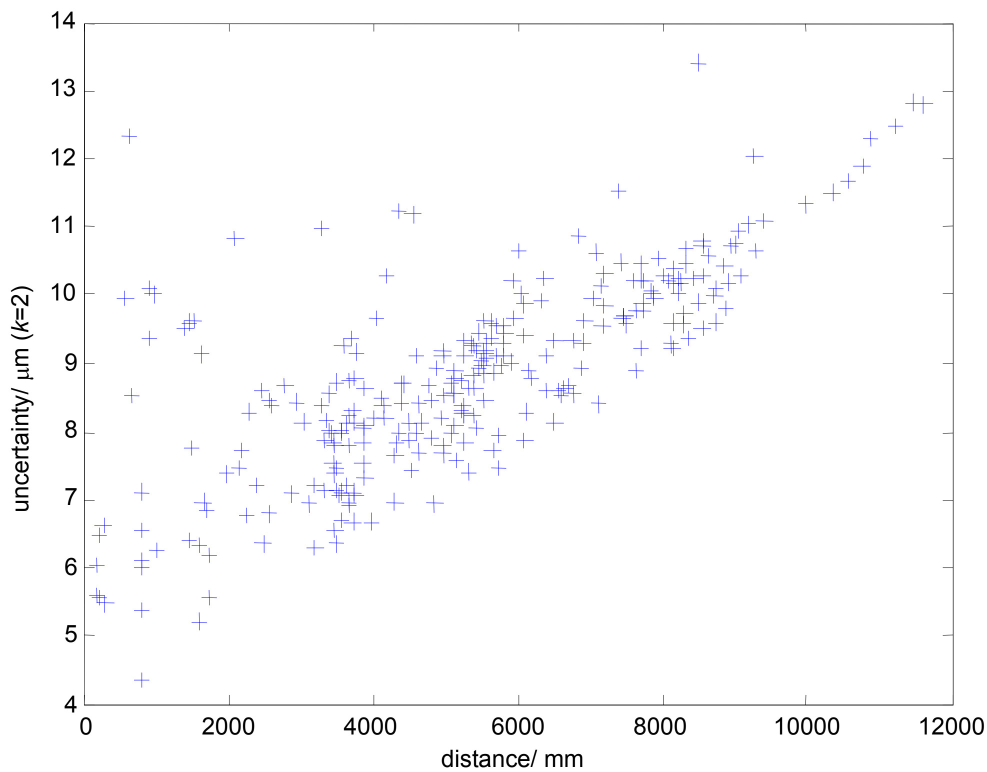

Figure 19. Expanded uncertainties (*k*=2) in micrometres associated with the inter-target distances plotted against distance in millimetres for the laser tracker survey.

4.1.2 iGPS measurement of reference points

The network of reference points was surveyed three times using the iGPS system with a mini vector bar. The vector bar was held by hand at each point until a stable measurement was obtained from the system. The angle data from this survey, together with the iGPS transmitter locations determined during the iGPS calibration phase were used in conjunction with the Metris "CORE" software to determine three sets Y_1, Y_2, and Y_3 of estimates of the coordinates of the reference points.

4.1.3 Laser Radar measurement of reference points

In addition to the above, the laser radar was used to survey the reference points. As with the laser tracker measurements, the laser radar surveys of the reference points were performed from multiple positions. The data was combined in the same way as for the laser tracker, using the same error model as for the laser tracker, to establish reference point coordinates Y_{R} and a variance matrix associated with the points. The residual errors associated with the distance, azimuth and elevation angles are given in Figure 20 to Figure 22. The expanded uncertainties associated with target coordinates for the laser radar survey are given in Figure 23. Although the accuracy of the laser tracker and laser radar displacement/distance and angle measurements are very similar, the tracker survey involved a total of 620 target measurements whereas the laser radar survey involved only 114 target measurements. This largely explains why the uncertainties in Figure 18 are smaller than those in Figure 23.

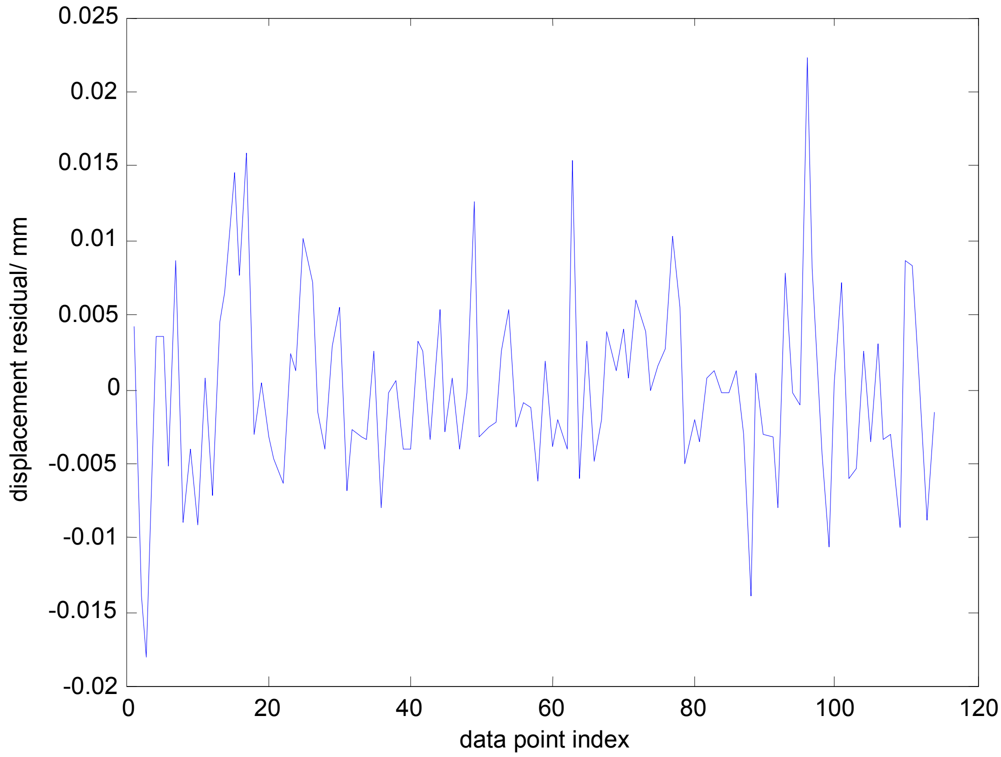

Figure 20. Residuals associated with the distance measurements for the laser radar survey in a least squares bundle adjustment.

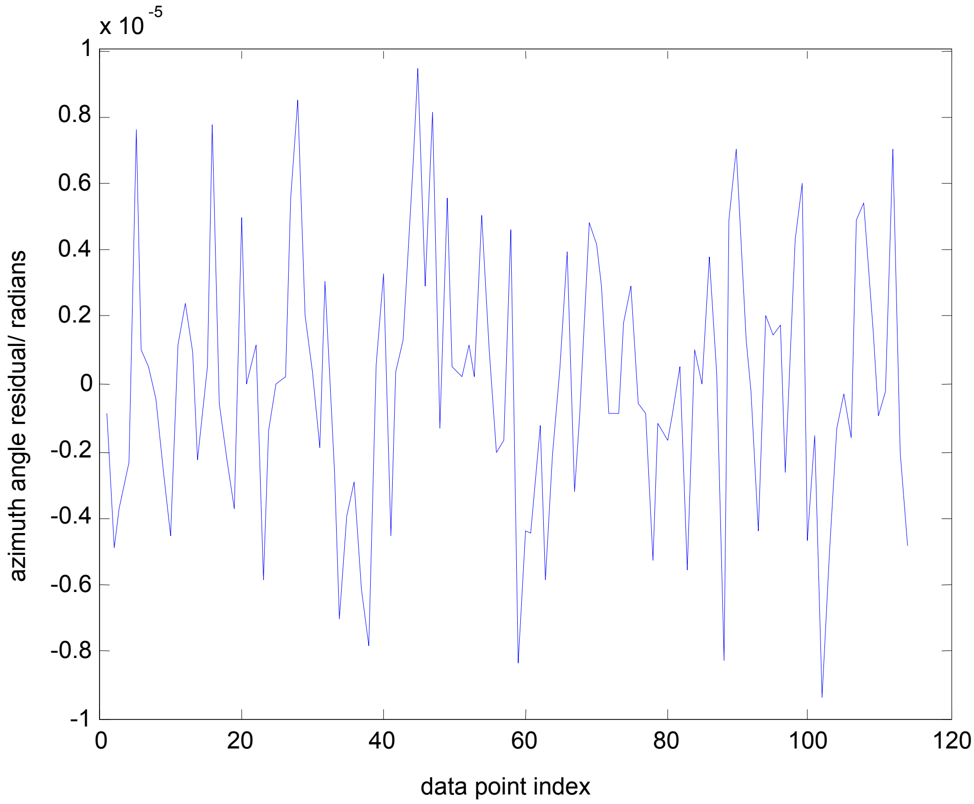

Figure 21. Residuals associated with the azimuth angle measurements for the laser radar survey in a least squares bundle adjustment.

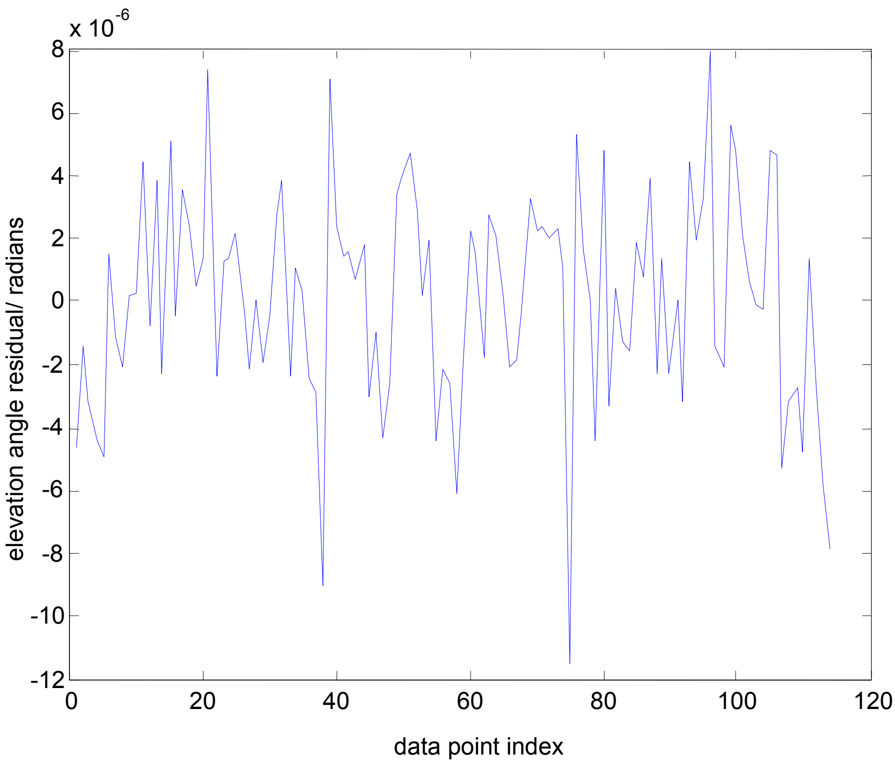

Figure 22. Residuals associated with the elevation angle measurements for the laser radar survey in a least squares bundle adjustment.

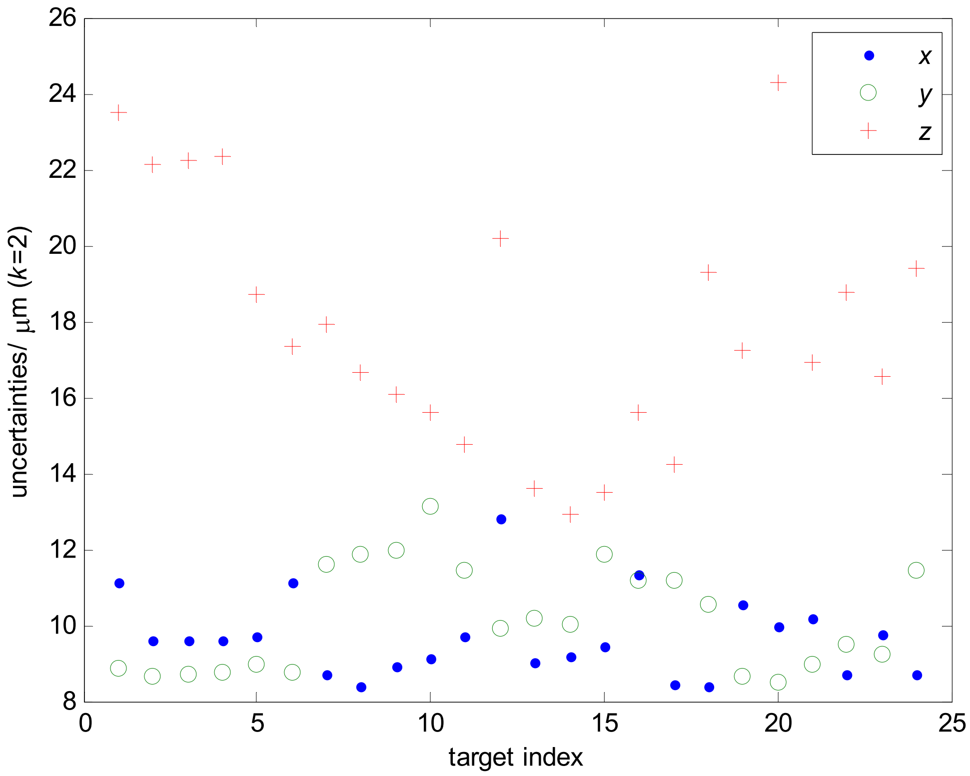

Figure 23. Expanded uncertainties (*k*=2) associated with the coordinates of the targets determined by the laser radar survey.

The uncertainty of the *z* coordinates of the targets obtained, *u(z)* using the laser radar survey is roughly a factor of 2 higher than the uncertainties obtained for *x* and *y*. This is because *u(z)* is dominated by the angular capability of the laser radar which is not as good as the range capability. For the *x* and *y* coordinates, the reverse applies. In the laser radar survey, the stations were located at one height and were position around the reference points whereas for the tracker survey two heights were used and some positions of the trackers were in the interior of the reference point locations. For this reason, the uncertainties associated with *z*-coordinates for the tracker measurements are more similar to those for the *x*- and *y*-coordinates; see Figure 18.

4.2 Comparison of data sets

From the measurements taken, five sets of estimates of the reference point locations where obtained, one from the tracker survey, a second from the laser radar and three from the iGPS system. The datasets were compared in terms of inter-point distances or as point clouds. In comparing point clouds, the different reference frames need to be taken into account. If a variance matrix associated with each data set is available, it can be used to weight the individual data points during the least-squares fitting processes so that more accurately known data points have more influence on the fitted result.

If variance matrices are not available, as was the case for the iGPS data, then a standard least squares matching method can be used. If $Y = \{\mathbf{y}_j, j = 1,\ldots,n\}$ and $Z = \{\mathbf{z}_j, j = 1,\ldots,n\}$ are two data sets representing measurements of the same set of targets (in the same order), then the standard least squares matching method determines the transformation parameters $\mathbf{t}$ defining the translation and rotation such that the transformed targets $\hat{\mathbf{z}}_j = \hat{\mathbf{z}}_j(\mathbf{t})$ minimises $\sum_{j=1}^{n} \left\| \mathbf{y}_j - \hat{\mathbf{z}}_j \right\|^2$.

4.2.1 *Comparison based on distances*

Differences between the calculated inter-point distances for the iGPS and laser tracker measurements are given in Figure 24 for the three sets of iGPS measurements. Over the three sets the mean difference (bias) is 42 µm with a standard deviation of 83 µm. The root mean squared error (the combination of the bias and standard deviation) is 93 µm. The graph shows no significant dependence on distance but does show a bias effect: on average the iGPS system is measuring longer than the laser tracker system.

The same type of comparison was made with the laser radar measurements; see Figure 25. The mean difference is 34 µm and the standard deviation is 85 µm.

The comparison between the laser radar distance measurements $d_{\mathrm{R},ij}$ and the laser tracker measurements $d_{\mathrm{T},ij}$ is presented in Figure 26. The figure shows some length dependency. The bundle adjustment software determines estimates of the variance matrices associated with the laser radar and laser tracker measurements, from which uncertainties $u(d_{\mathrm{R},ij})$ and $u(d_{\mathrm{R},ij})$ in the inter-point distances were calculated. The laser radar and laser tracker systems were regarded as statistically independent, and the uncertainty $u(\Delta_{ij})$ in the difference $\Delta_{ij} = d_{\mathrm{R},ij} - d_{\mathrm{T},ij}$ was estimated by $u^2(\Delta_{ij}) = u^2(d_{\mathrm{R},ij}) + u^2(d_{\mathrm{T},ij})$. Figure 27 plots the normalised differences $\Delta_{ij} / u(\Delta_{ij})$; again some scale effect can be seen. Figure 28 plots the normalised difference but for the case where the laser radar distances have been reduced by 2 parts per million (ppm). With this scaling, the differences were more in line with those predicted by the statistical model, which would require 95 % of points to lie within the region ± 2.

This analysis shows that the laser radar and laser tracker data sets and their associated uncertainty models are entirely consistent with the observed behaviour. This confirms that the models and data can be used with high confidence and that either instrument is suitable for calibration of the iGPS monuments. The 2 ppm scale difference between the two instruments is not considered to be relevant for this experiment.

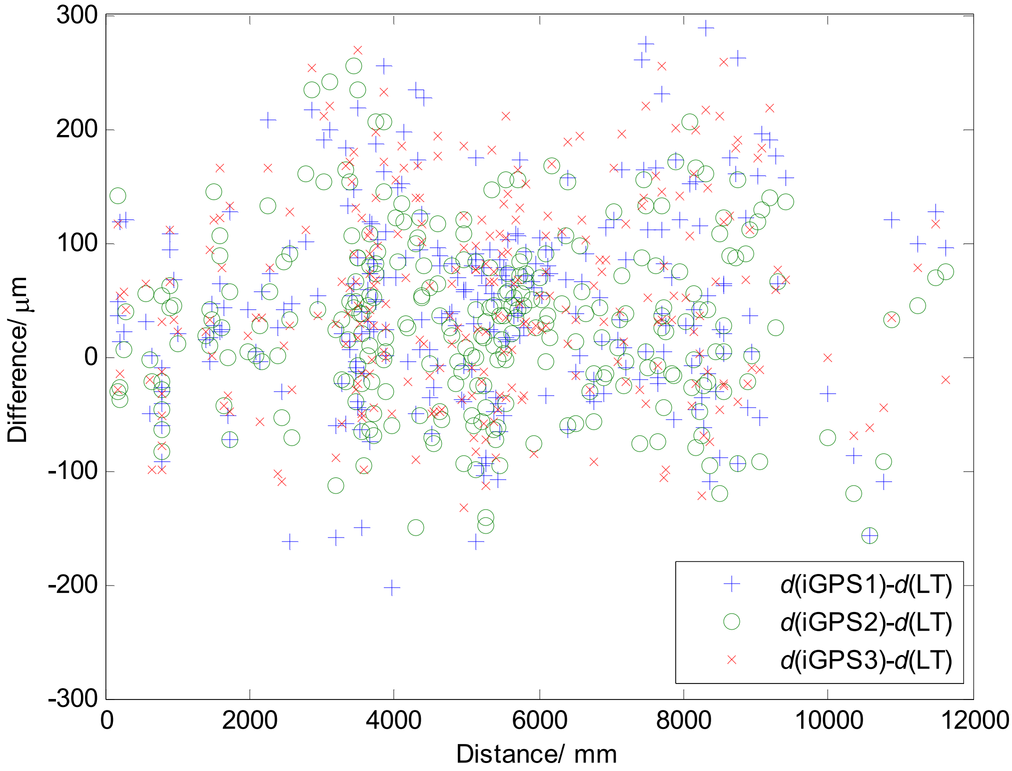

Figure 24. Differences between the inter-point distances for the iGPS and laser tracker measurements, calculated for the three iGPS sets of target estimates.

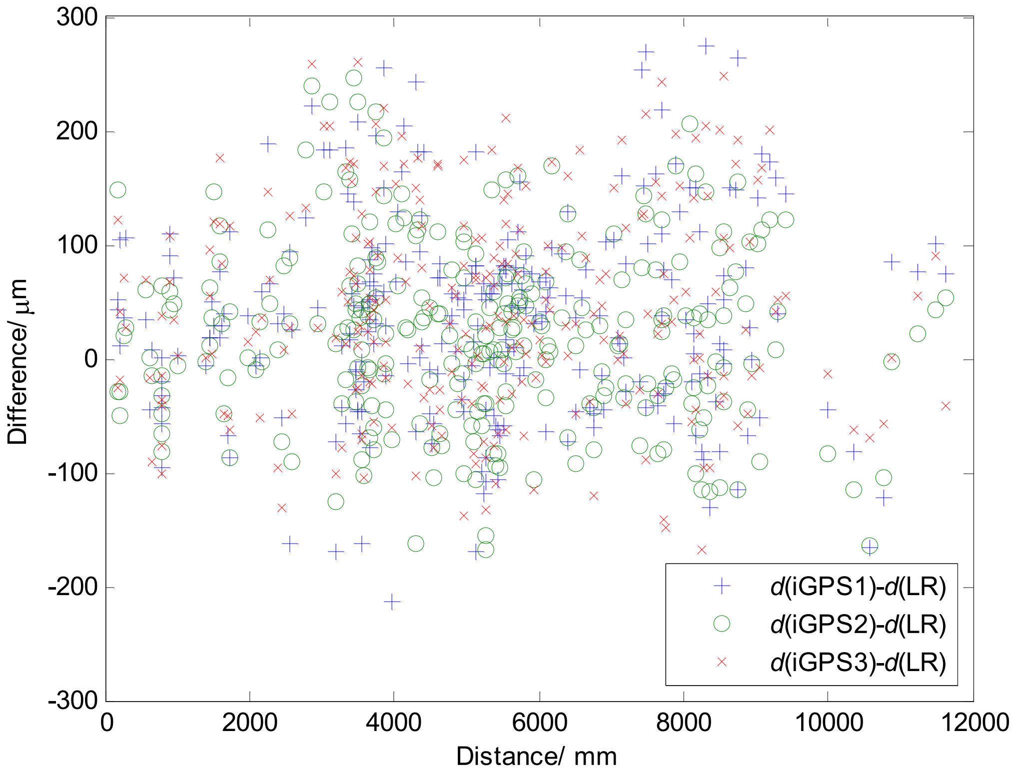

Figure 25. Differences between the inter-point distances for the iGPS and laser radar measurements, calculated for the three iGPS sets of target estimates.

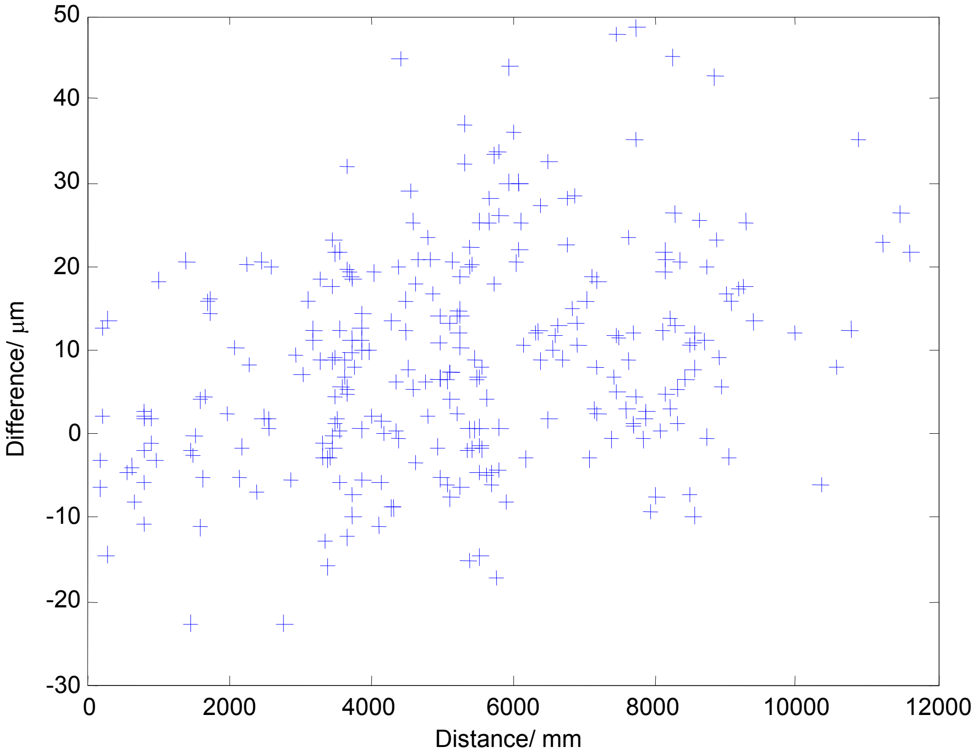

Figure 26. Difference between the laser radar distances and the laser tracker distances.

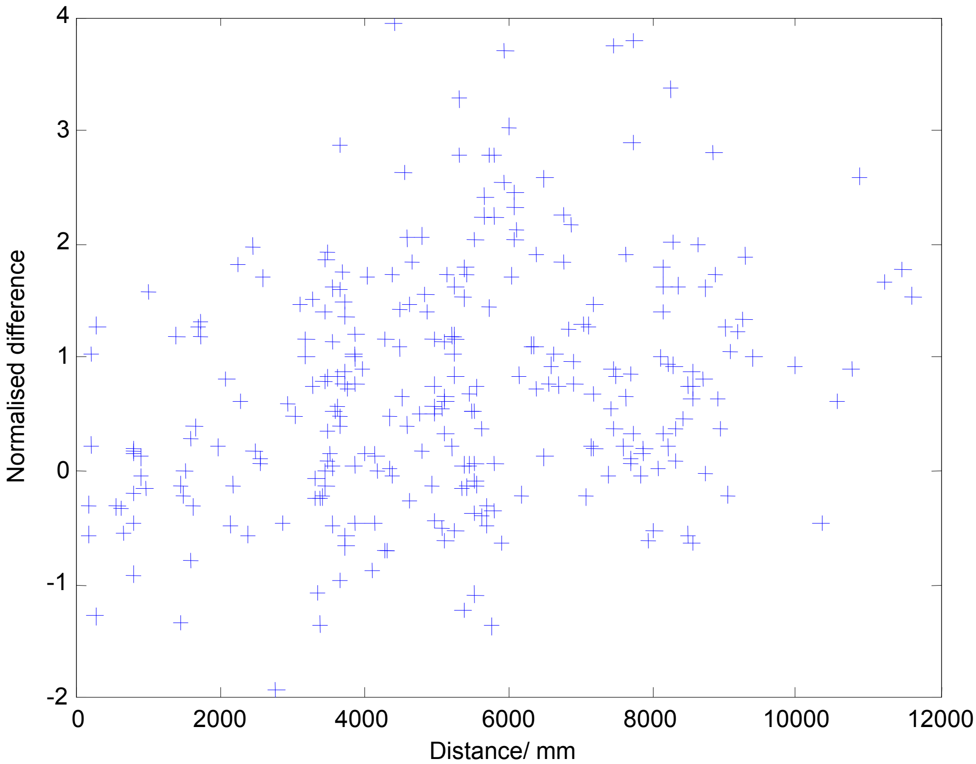

Figure 27. Normalised differences between the laser radar and laser tracker distance measurements.

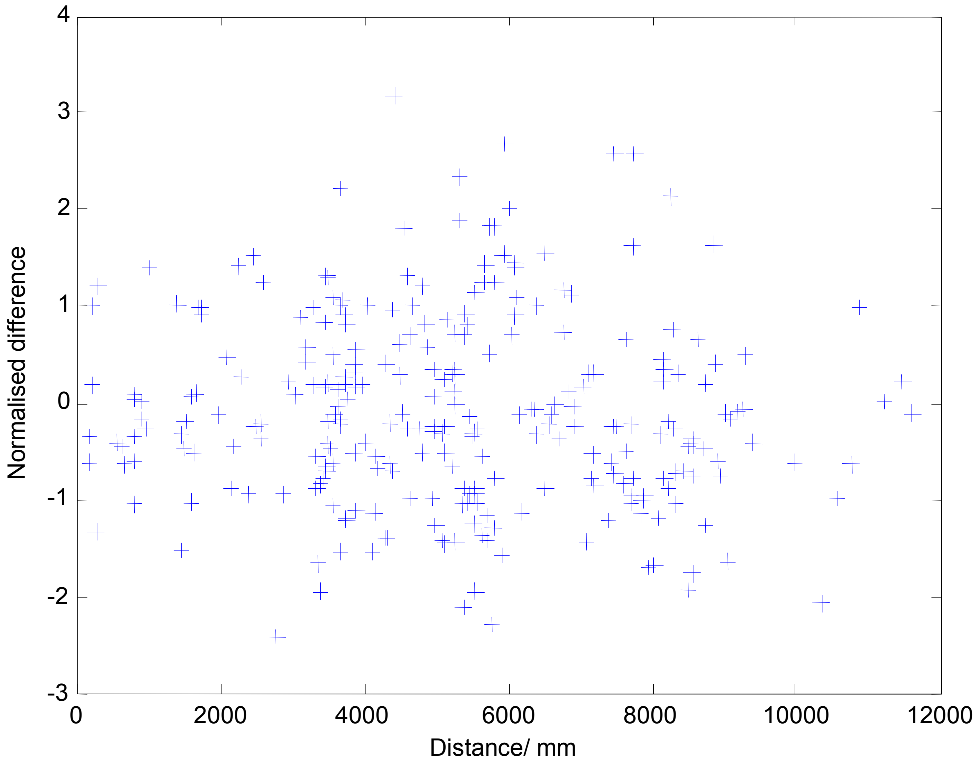

Figure 28. Normalised differences between the laser radar and laser tracker distance measurements, with the laser radar distances reduced by a factor of 2 parts per million.

4.2.2 Comparison based on point coordinates

Figure 29 to Figure 31 give the difference in coordinates between the iGPS measurements and the laser tracker measurements calculated using a standard least squares matching algorithm with no weighting. Y_1, Y_2 and Y_3 represent three measurements of the same set of targets acquired by iGPS system. Y_T and Y_R represent the laser tracker and laser radar measurement respectively. Across the three data sets, the standard deviation of the difference is approximately 0.060 mm for the *x*- and *y*-coordinates and approximately 0.095 mm for the *z*-coordinate. For comparison, the differences between the laser radar measured coordinates and those from the laser tracker survey are given in Figure 32. The differences are approximately in line with those predicted by the uncertainty models for the laser tracker and laser radar measurements, with the possible exception of the heights associated with reference points 3, 18 and 19. The uncertainty model assumes that both systems were measuring exactly the same set of reference points. In practice, there is likely to be some change in point location between the two sets of measurements. If we include a random change with standard deviation 0.007 mm in each coordinate between the two sets of measurements, the two sets of measurements are consistent with the (adjusted) uncertainty model.

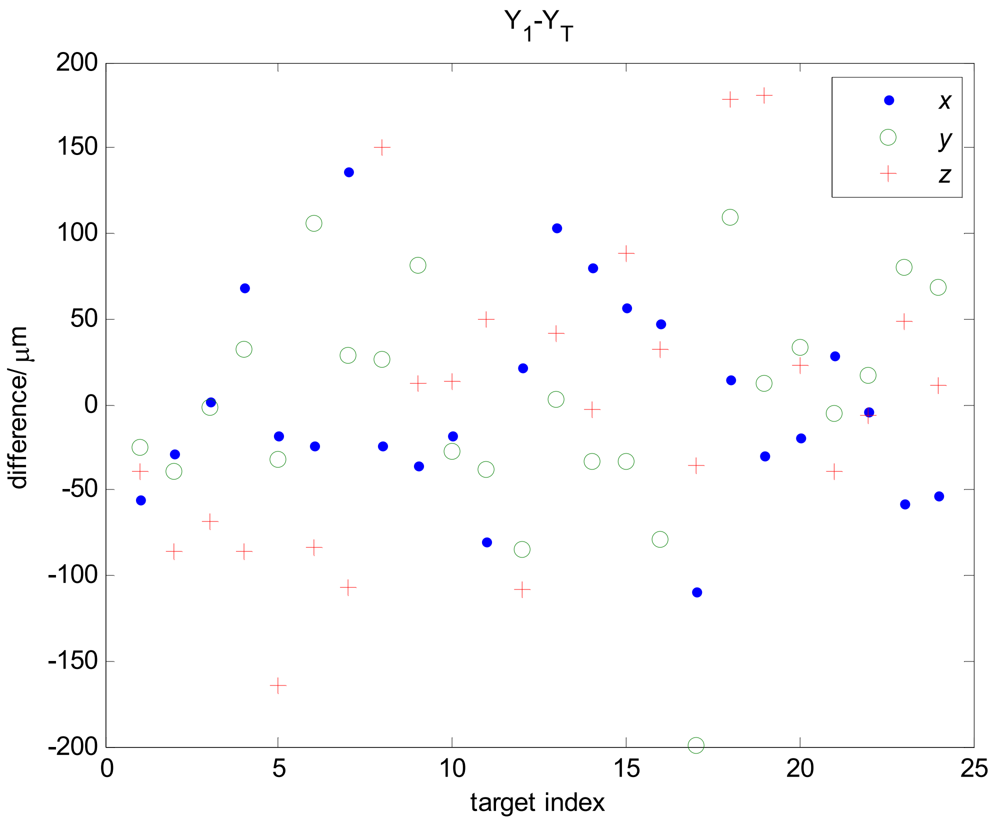

Figure 29. Comparison of coordinates set Y_1 and Y_T calculated using the standard least squares matching algorithm.

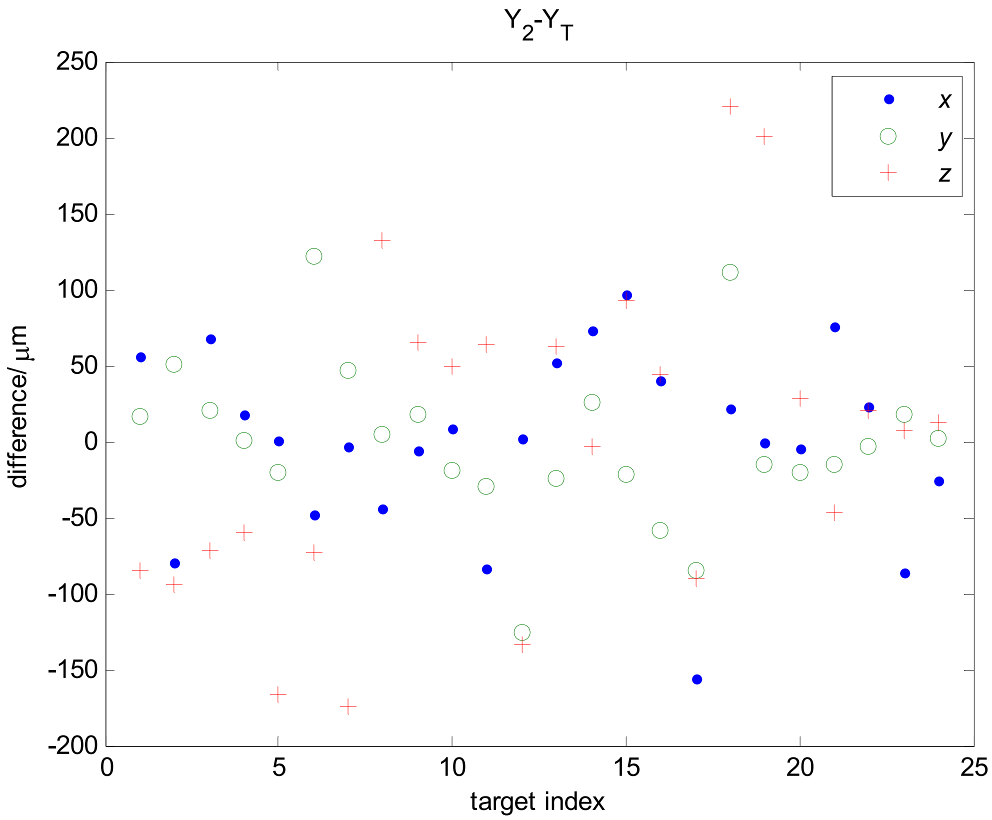

Figure 30. Comparison of coordinates set Y_2 and Y_T calculated using the standard least squares matching algorithm.

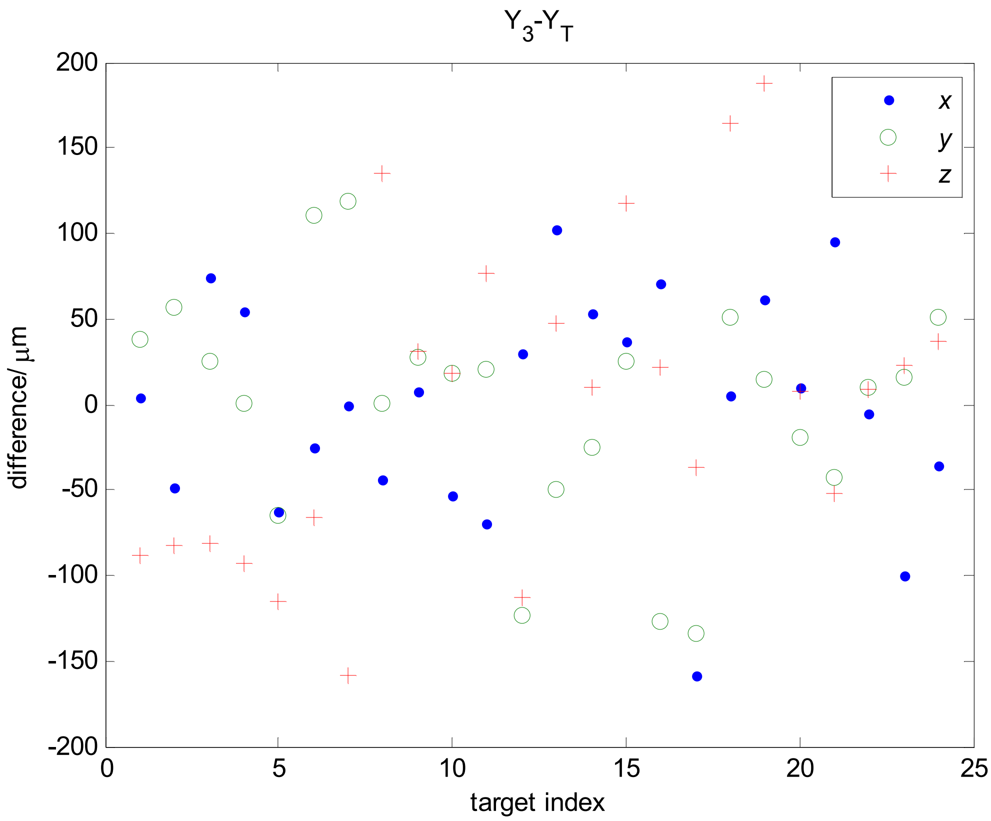

Figure 31. Comparison of coordinates set Y_3 and Y_T calculated using a standard least squares matching algorithm.

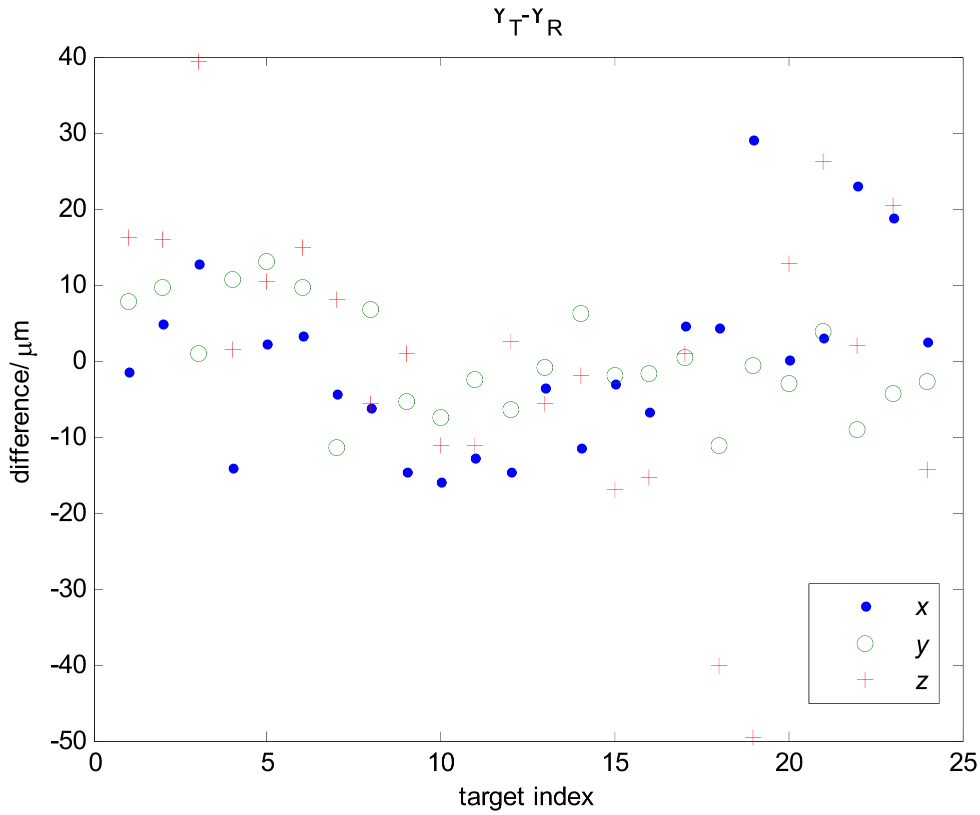

Figure 32. Comparison of coordinate set Y_R (laser radar) and Y_T (laser tracker) calculated using the standard least squares matching algorithm.

The notable feature in the differences between the laser tracker results and the iGPS data is that they are similar for the *x*, *y* and *z* coordinates. This is in contrast to the behaviour predicted by the uncertainty model described in section 2.1 which predicted that the uncertainty in *z* would be significantly lower than that in *x* and *y*.

This difference between observed behaviour and that predicted by the model illustrate that the iGPS system is, in fact, more complex than the simple model used here.

4.2.3 iGPS measurements compared

The three sets of iGPS measurements can be compared with each other; Figure 29, Figure 30 and Figure 31 show the pair-wise difference in coordinates. The standard deviation for the difference in *x*- and *y*-coordinates is approximately 0.050 mm and that for the *z*-coordinate 0.035 mm.

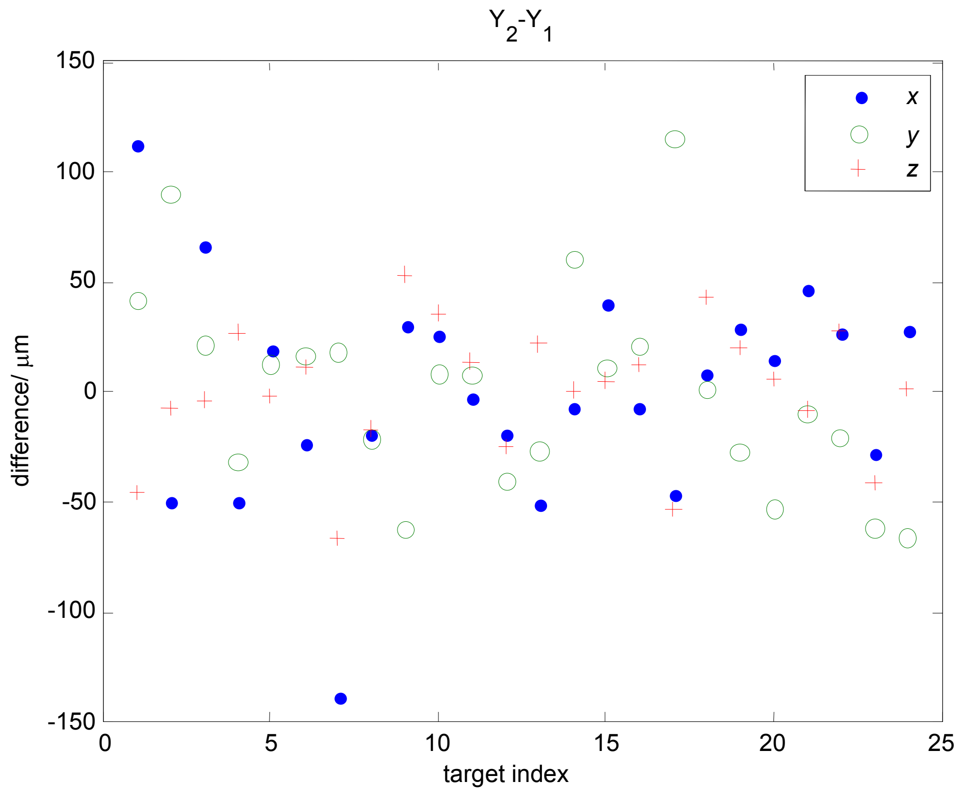

Figure 33. Comparison of iGPS coordinate sets Y_2 and Y_1 calculated using the standard least squares matching algorithm.

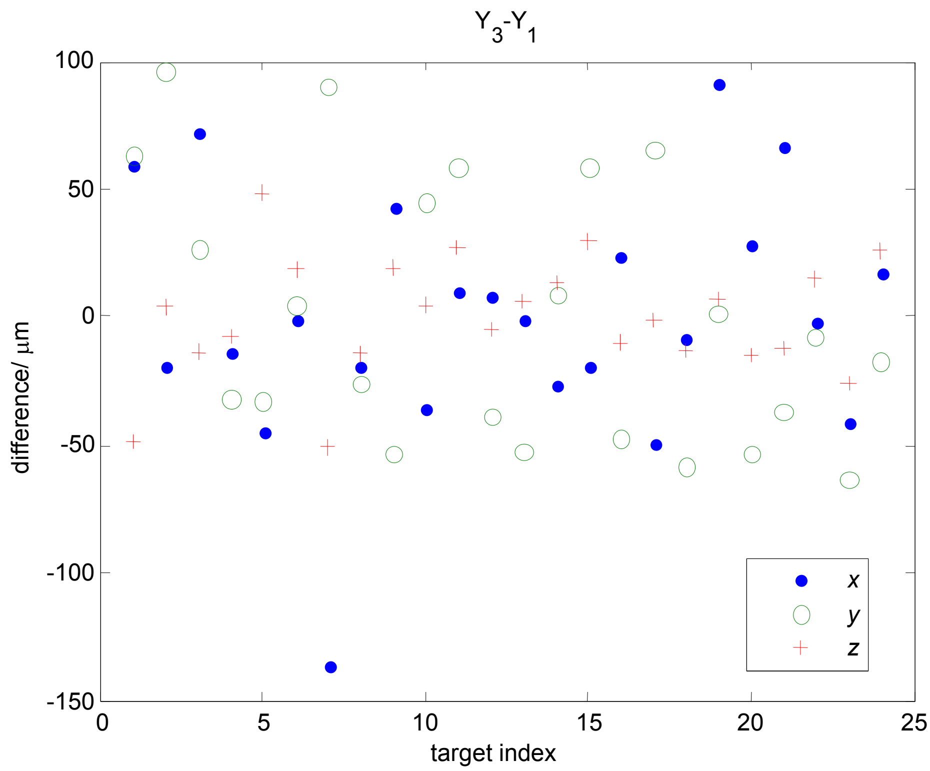

Figure 34. Comparison of iGPS coordinate sets Y_3 and Y_1 calculated using the standard least squares matching algorithm.

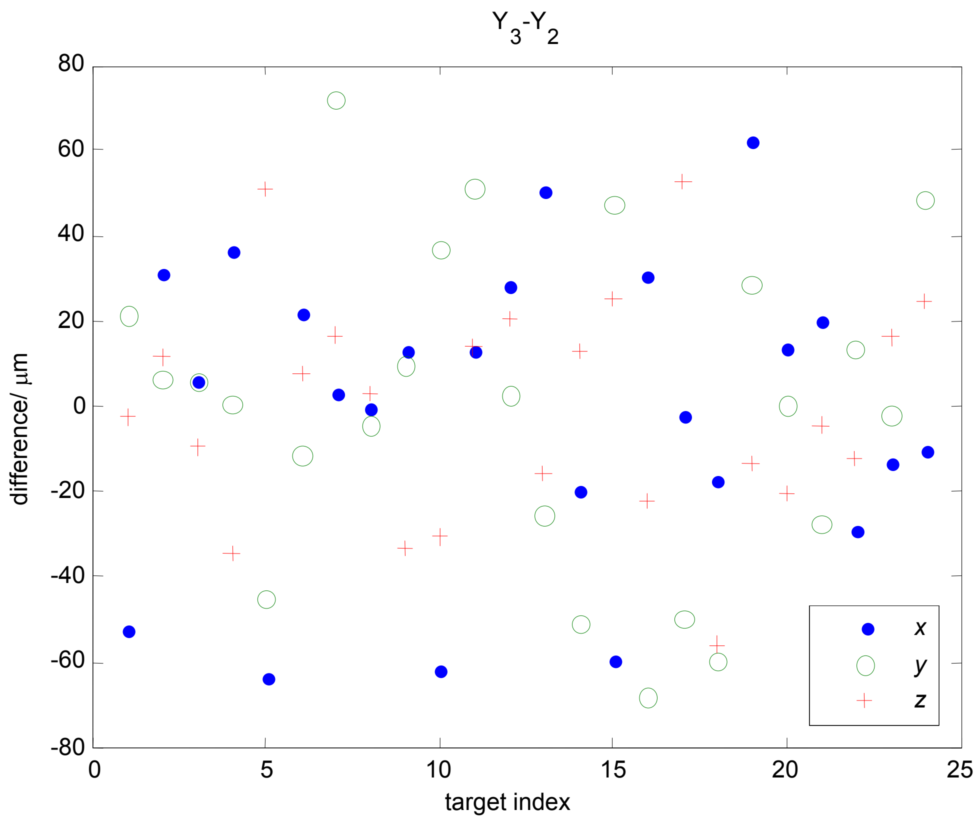

Figure 35. Comparison of iGPS coordinate sets Y_3 and Y_2 calculated using the standard least squares matching algorithm.

4.3 Scale Bar Tests

The mean length of the scale bar as measured by the iGPS system was calculated to be 1551.692 mm. The deviations from the mean for the 29 individual measurements are plotted in Figure 36 below. The standard deviation of these measurements was 57.4 µm.

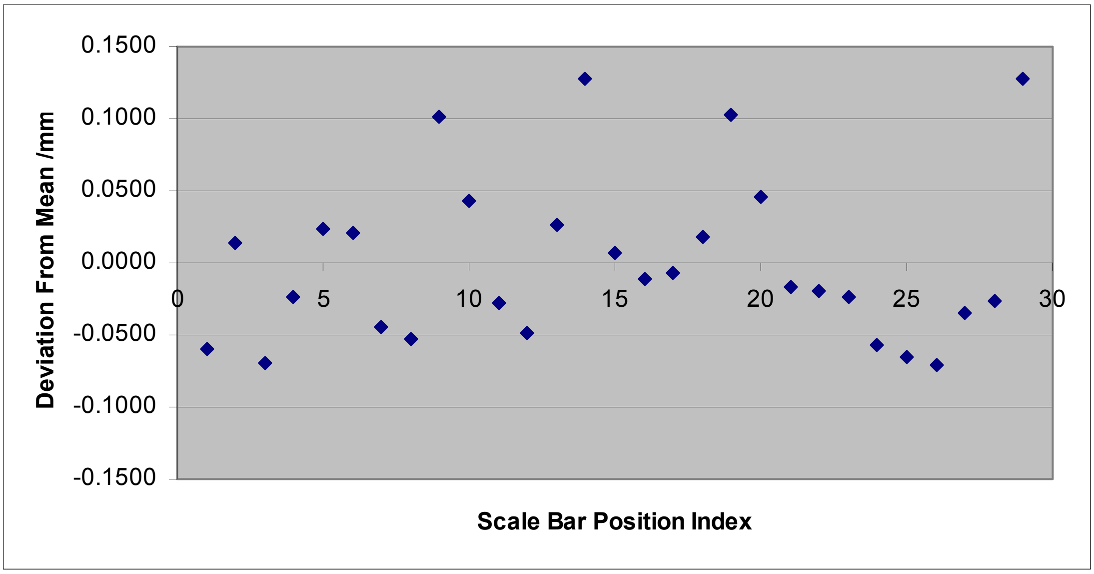

Figure 36. Variation in scale bar readings for different scale bar positions.

The data was further processed to investigate any correlation between measured length and orientation within the measurement volume. The variation in measured length with rotation around the *x*-, *y*-, and *z*-axes are shown in the graphs of Figure 37 to Figure 39.

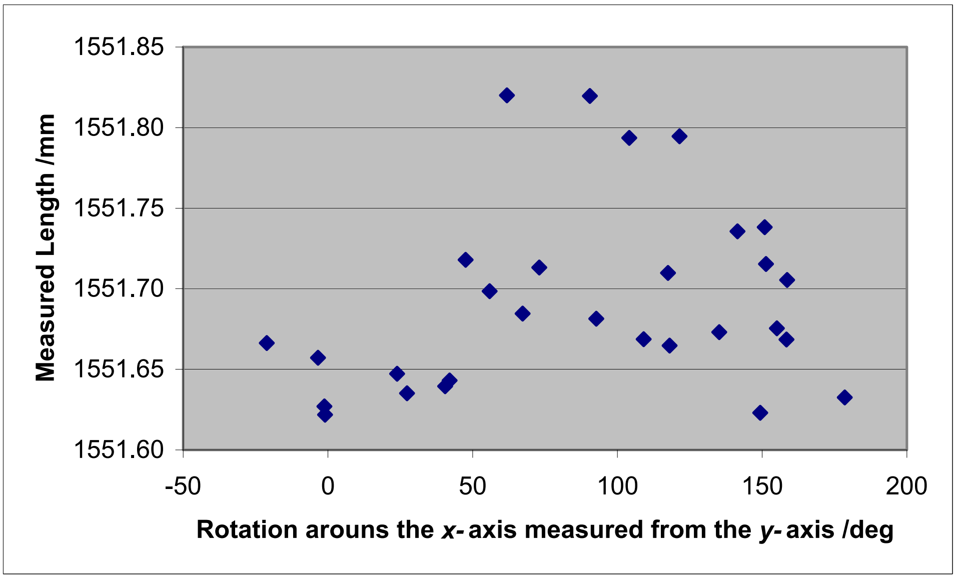

Figure 37. Variation in measured length of the scale bar with rotation around the *x*-axis.

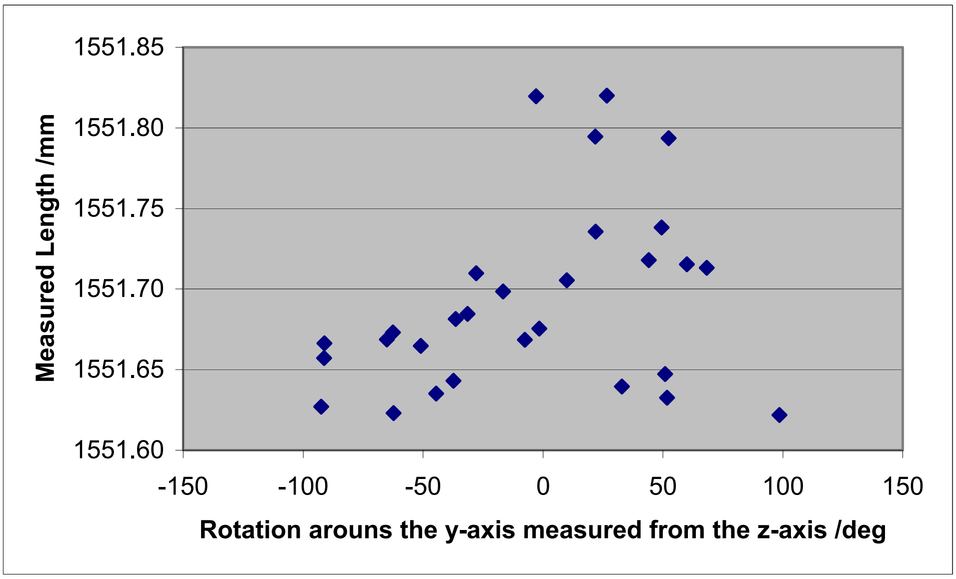

Figure 38. Variation in measured length of the scale bar with rotation around the *y*-axis.

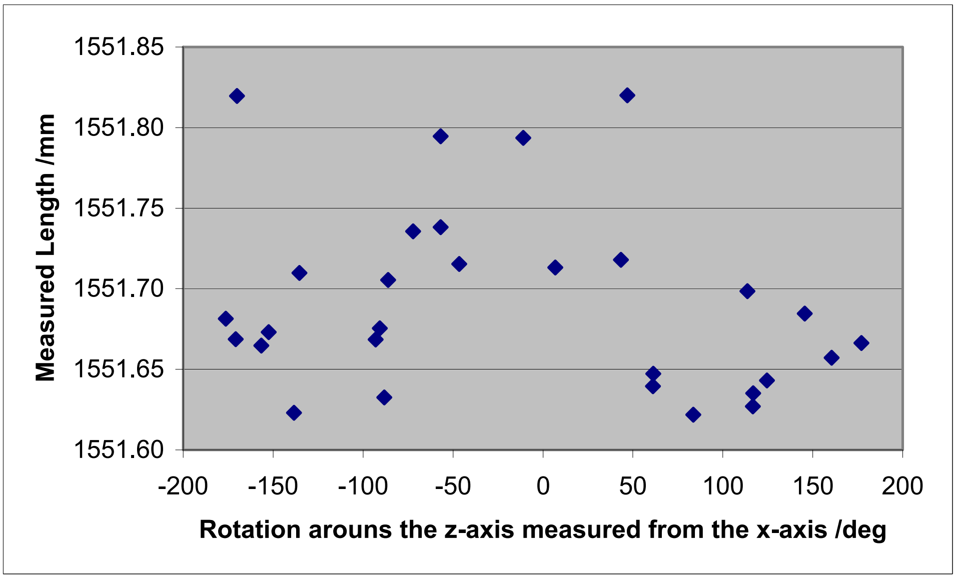

Figure 39. Variation in measured length of the scale bar with rotation around the *z*-axis.

These graphs show no apparent correlation between the orientation of the vector bar and the measured length.

5 Discussion

5.1 Discrepancy between uncertainty models and observed behaviour

The uncertainty model developed by NPL for the iGPS system caters for: random effects associated with the sensor measurements (taken to be measurements of azimuth and elevation angle); systematic effects accounting for the measuring station positions and orientations, and calibration information relating to scale bars, monument positions and vector bar geometry. On the basis of this model, it is predicted that the iGPS system should measure the z-coordinate more accurately than the *x*- and *y*-coordinates. When we compare the iGPS measurements with the laser tracker (or laser radar) measurements, we find that the z-coordinate is less accurately determined than the x- and y-coordinates. Following discussions with Metris, we believe that the reason for this discrepancy is due to systematic effects associated with the calibration of the transmitter-receiver pairs that are not accounted for by the uncertainty model.

Comparing the three sets of iGPS measurements with themselves, we find that the variation in the z-coordinate is, indeed, less than that for the x- and y-components. Since these variations are likely to be due to random effects, this behaviour can be explained in terms of the reference uncertainty model. The observed variations are consistent with the uncertainty model described in section 2.1 with $\sigma_A = 0.35$ arcseconds and $\sigma_B = 0.035$ mm.

The overall behaviour of the iGPS system can be approximately modelled by the uncertainty model with $\sigma_A = 1$ arcsecond and $\sigma_B = 0.150$ mm. However, this model underestimates the uncertainty associated with the z measurements and overestimates the uncertainties associated with short measuring lengths (where the systematic effects are likely to be correlated). This is evident when comparing the standard deviation of the scale bar measurements with that of the inter-point distances. The scale bar was approximately 1.5 m in length compared to the 12 m range of inter-point lengths measured and the standard deviations were 57 μm and 85 μm respectively.

5.2 Project deliverables

The difficulty in accounting for systematic effects in the uncertainty model has meant that it would be difficult to use the uncertainty model as a basis of a good practice guide for iGPS/iSPACE measurement. Furthermore, the iGPS system has been upgraded during the course of the project. In the run-up to performing the experimental work in March 2008, Metris introduced a new variant of iGPS and software referred to as iSPACE. The iSPACE system provided by Metris for testing was a monument-based configuration. The system was calibrated using the monuments that were themselves calibrated by surveying with a laser radar survey. In a monument-based configuration the position of the vector bar is continously calculated with reference to the monument locations with the transmitter positions continually updated as part of the calculation. (This approach has many potential advantages.)

The monument setup was not included in the original reference model and additional model development was required to enable us to analyse the data appropriately. This extra work could only be accommodated within the schedule and financial constraints of the project at the expense of other deliverables, namely the good practice guide. This change in the deliverables was agreed by Airbus, the main industrial partner in the project.

In addition, the relatively simple model of the iGPS system developed during this work is not representative enough of the real system to allow accurate predictions of performance to be made – as described above the observed measurement deviation does not agree with the model predicted uncertainty, particularly the z coordinates. Further work is required to develop models that take into account systematic effects so that more reliable uncertainty evaluations can be made.

To address this shortfall in the deliverables, NPL has secured funding from a European (EMRP) project to continue the modelling/data analysis work and to produce a good practice guide. This work is due to be completed in 2010.

Consequently, the results described here represent the performance of the particular iGPS/iSPACE system that was tested and is not representative of all possible setups.

6 Conclusions

An experiment was performed to determine the performance of the Metris Indoor GPS system by comparison with a reference system based on two laser trackers operated in a multilateration mode. A system of reference points was set up and surveyed using laser trackers. The reference points were also surveyed using a laser radar and the iGPS system under test. The reference coordinates and inter-point lengths were calculated from the laser tracker data using a robust, weighted least squares fitting algorithm. Some outliers were removed prior to fitting. The uncertainties associated with the reference point measurements were calculated based on an uncertainty model for the laser tracker. The residuals of this fit showed good consistency between data and model.

The same process was repeated for the laser radar survey data. The laser radar and laser tracker data were then compared. The analysis showed that (after a slight adjustment for laser radar scale of 2 ppm) the uncertainty models associated with these instruments were largely consistent with the observed behaviour. There is evidence that the heights of some of the reference points had changed over the course of the measurements.

Additionally, the reference point coordinates obtained using the laser tracker were compared with the same points measured by the iGPS system using a standard least-squares fitting process.

This comparison showed that standard deviation of differences between the two systems for inter-point distances up to 12 m was 0.085 mm with a maximum observed difference of 0.290 mm. The standard deviation of the difference in x- and y-coordinates was 0.060 mm while that of the z-coordinate 0.095 mm. The maximum observed difference were 0.160 mm for x, 0.200 mm for y and 0.220 mm for z. These results are summarised in Table 1.

	d	x	y	z
std/mm	0.085	0.060	0.060	0.095
max/mm	0.290	0.160	0.200	0.220

Table 1. Differences between the iGPS measurements and the laser tracker measurements for distances and coordinates.

Comparison between the observed results and those predicted by the simple uncertainty model used to represent the iGPS system show that the model adequately predicts actual behaviour in the x and y directions but overestimates the accuracy in the z direction. Some possible improvements to the model that may help explain these discrepancies are listed below:

- Account for systematic effects through correlation between observations along similar lines of sight.

- Investigate the actual Cartesian miss reported by the iGPS software to see if the behaviour can provide insight into the uncertainty model.

A NMS/EMRP funded project will investigate this further and develop the uncertainty model to a stage where it can more reliably predict system performance.

Acknowledgements
The authors wish to express their thanks to Metris, in particular Roger Holden, Chris Cartile and Tom Hedges for providing the equipment used in the tests and for their expert knowledge and insight into the operation of the iGPS system; and to Geraint Jones and Mike O’Sullivan at Airbus, Broughton and Mark Summers and Amir Kayani at Airbus, Filton, respectively for providing the location for the work and loan of a laser tracker and cash funding.

7 References

[1] G N Peggs, P G Maropoulos, E B Hughes, A B Forbes, S Robson, M Ziebart, and B Muralikrishnan. “Recent developments in large-scale dimensional metrology”, Proc. ImechE Vol. 223 Part B: J. Engineering Manufacture, 2009, p571-595.

[2] Forbes, A. B. and Harris, P. M. ”Uncertainty associated with co-ordinate measurements”, Laser Metrology and Machine Performance {VII}, Bedford 2005, Euspen, p30-39.

[3] Forbes, A. B., “Evaluation of {CMM} measurements of hole plates in interlaboratory comparisons”, Laser Metrology and Machine Performance {VII}, Bedford, 2007, Euspen, p368-377.